

# Basin inversion and structural architecture as constraints on fluid flow and Pb–Zn mineralisation in the Paleo–Mesoproterozoic sedimentary sequences of northern Australia

George M. Gibson<sup>1</sup>

<sup>1</sup>Research School of Earth Sciences, Australian National University, Canberra ACT 2601, Australia

Sally Edwards<sup>2</sup>

<sup>2</sup>Geological Survey of Queensland, Department of Natural Resources, Mines and Energy, Brisbane, Queensland 4000, Australia

Correspondence to: George M. Gibson (George.gibson@anu.edu.au)

## Abstract

As host to several world-class sediment-hosted Pb–Zn deposits and unknown quantities of conventional and unconventional gas, the variably inverted 1730–1640 Ma Calvert and 1640–1575 Ma Isa superbasins of northern Australia have been the subject of numerous seismic reflection studies with a view to better understanding basin architecture and fluid migration pathways. These studies reveal a structural architecture common to inverted sedimentary basins the world over, including much younger examples known to be prospective for oil and gas in the North Sea and elsewhere, and with which they might be usefully compared. Such comparisons lend themselves to suggestions that the mineral and petroleum systems in Paleo–Mesoproterozoic northern Australia may have spatially, if not temporally overlapped and shared a common tectonic driver, consistent with the observation that basinal sequences hosting Pb–Zn mineralisation in northern Australia are bituminous or abnormally enriched in hydrocarbons. Sediment-hosted Pb–Zn mineralisation coeval with basin inversion first occurred during the 1650–1640 Ma Riversleigh Tectonic Event towards the close of the Calvert Superbasin with further pulses taking place during and subsequent to onset of the 1620–1580 Ma Isa Orogeny and final closure of the Isa Superbasin. Mineralisation is typically hosted by the post-rift or syn-inversion fraction of basin fill, contrary to existing interpretations of Pb–Zn ore genesis where the ore-forming fluids are introduced during the rifting or syn-extensional phase of basin development. Mineralising fluids were instead expelled upwards during times of crustal shortening into structural and/or chemical traps developing in the hangingwalls of inverted normal faults. Inverted normal faults predominantly strike NNW and ENE, giving rise to a complex architecture of compartmentalised sub-basins whose individual uplifted basement blocks and doubly-plunging periclinal folds exerted a strong control not only on the distribution and preservation of potential trap rocks but the direction of fluid flow, culminating in the co-location and trapping of mineralising and hydrocarbon fluids in the same carbonaceous rocks. An important case study is the 1575 Ma Century Pb–Zn deposit where the carbonaceous host rocks served as both a reductant and basin seal during the influx of more oxidised mineralising fluids, forcing the latter to give up their Pb and Zn metal. A transpressive tectonic regime in which basin inversion and mineralisation were paired to folding, uplift and erosion during arc-continent or continent-continent collision, and accompanied by orogen-parallel extensional collapse and strike-slip faulting best accounts for the observed relationships.

## 1 Introduction

40 Northern Australia and its late Paleoproterozoic–early Mesoproterozoic basinal sequences have long  
41 attracted the interest of the minerals and petroleum exploration industries. Besides being the world’s single  
42 largest repository of sediment-hosted Pb–Zn mineral deposits (Huston et al., 2006;Southgate et al., 2006),  
43 these same mineral-rich sequences hold some of the planet’s oldest oil (Jackson et al., 1986) along with an  
44 unknown quantity of conventional and unconventional gas (Carr et al., 2019;Gorton and Troup,  
45 2018;McConachie et al., 1993). Unsurprisingly, many mineral deposits and their host rocks are bituminous  
46 or contain very high proportions of organic carbon (Andrews, 1998;Broadbent et al., 1998;Hutton and  
47 Sweet, 1982;Jarrett et al., 2018;McConachie et al., 1993;McGoldrick et al., 2010), raising the possibility  
48 that the petroleum and mineralising systems in northern Australia may have spatially, if not temporally,  
49 overlapped and share a common tectonic driver. Such a possibility was first entertained for the ca. 1575 Ma  
50 Century Pb–Zn deposit (Fig. 1a) where first hydrocarbons and then a more metalliferous ore-forming fluid  
51 are thought to have been sequentially trapped following their expulsion from deeper stratigraphic levels  
52 during folding and thrusting accompanying the 1620–1580 Ma Isan Orogeny (Broadbent et al., 1998). In  
53 this scenario, basin inversion was not only intimately linked to fluid migration and mineralisation but played  
54 a key role in generating the structural architecture that brought the petroleum and mineralising systems  
55 together in one place. Seismic reflection images for the Lawn Hill Platform have since shown the Century  
56 deposit to be hosted by the syn-inversion fraction of basin fill (Gibson et al., 2017;Gibson et al., 2016) and  
57 occur in rocks possessing a structural architecture common to inverted basins the world over, including  
58 those currently under exploration for oil and gas in the Irish and North seas and north European continental  
59 shelf more generally (Cooper et al., 1984;Hayward and Graham, 1989;Lowell, 1995;Thomas and Coward,  
60 1995;Turner and Williams, 2004). Thus, not only does basin inversion appear to have been a prerequisite  
61 for ore formation at Century, but the structural architecture cannot have appreciably changed during the  
62 transition from a hydrocarbon to mineral system lest the similarities with their more modern European  
63 counterparts have been lost during crustal shortening. Such conclusions are difficult to reconcile with most  
64 existing models for sediment-hosted Pb–Zn mineralisation in northern Australia where ore formation is  
65 interpreted to have been syn-extensional and facilitated by fluid migration along normal faults active at the  
66 time of basin formation (Huston et al., 2006;Large et al., 2005;Leach et al., 2010;McGoldrick et al., 2010).  
67 Alternative exploration strategies for this and other types of sediment-hosted Pb–Zn mineralisation in  
68 northern Australia may therefore be warranted that better reflect the similarities with the petroleum system  
69 and target the structures formed during basin inversion. Here, we make use of publically available industry  
70 and government deep seismic reflection data to show that inversion-related structures of more than one  
71 generation and style are widely developed in the late Paleoproterozoic–early Mesoproterozoic basin  
72 sequences of northern Australia (Figs. 1 & 2), reflecting successive episodes of crustal shortening during  
73 the course of which the majority of Pb–Zn deposits were emplaced (Gibson et al., 2017).

## 74 **2 Regional geology and basin-forming events of northern Australia**

75 Northern Australia’s late Paleoproterozoic–early Mesoproterozoic basinal sequences belong to one of three  
76 superbasins (Figs. 2 & 3) which, together with the overlying Mesoproterozoic South Nicholson Basin (Fig.  
77 1a), preserve a 500 million year history of lithospheric extension interrupted by successive episodes of  
78 basin inversion, uplift and erosion (Betts et al., 2016;Gibson et al., 2012;Giles et al., 2002;Jackson et al.,  
79 2000;Neumann et al., 2006;Southgate et al., 2000a;Sweet, 2017;Yang et al., 2020). The oldest basin  
80 inversion event (Fig. 3) occurred after 1840 Ma and is best expressed by the angular unconformity  
81 separating the 6–8 km thick 1790–1740 Ma Leichhardt Superbasin (Fig. 2) from an older underlying  $\geq 1870$   
82 Ma crystalline basement (Kalkadoon-Leichhardt Block; Fig. 2) variably intruded by foliated 1860–1840  
83 Ma granites (Blake, 1987;Withnall and Hutton, 2013). Clasts of strongly foliated granite and other basement  
84 rocks occur widely in conglomerates at the base of the Leichhardt Superbasin (1790 Ma Bottletree  
85 Formation) but otherwise its basin fill is only mildly deformed and mainly comprises weakly

86 metamorphosed (greenschist facies) continental tholeiites and rhyolite interstratified with subordinate but  
87 still substantial volumes of fluviatile-shallow marine sedimentary rocks. This same cover-basement  
88 relationship is also evident on the Murphy Ridge (Fig. 4) farther north where conglomerates (Westmoreland  
89 Conglomerate) and sandstones (Wire Creek Sandstone) at the base of the 1790–1710 Ma Tawallah Group  
90 (Fig. 3) in the McArthur Basin (Fig. 1b) similarly rest unconformably on an older deformed basement  
91 intruded by 1860–1840 Ma granites (Ahmad and Munson, 2013; Rawlings et al., 2008; Sweet, 1984). As  
92 with the Kalkadoon-Leichhardt Block, basement granites on the Murphy Ridge were deformed long before  
93 the overlying conglomerate was deposited and likely represent exposed fragments of a much more  
94 regionally extensive magmatic belt that is continuous at depth and once lay at or close to the eastern margin  
95 of the North Australian Craton (Gibson et al., 2008; Korsch et al., 2012). Granites with calc-alkaline  
96 compositions occur widely throughout the Kalkadoon-Leichhardt Block (Bierlein et al., 2011) and may  
97 originally have formed part of a continental magmatic arc linked to west-dipping subduction beneath the  
98 eastern margin of the craton (Bierlein et al., 2008; Korsch et al., 2012). Alternatively, these granites  
99 originated in a backarc setting linked to oceanward retreat of a more distal arc built along either the southern  
100 or eastern margin of conjoined North and South Australian cratons (Betts et al., 2016; Betts and Giles,  
101 2006; Gibson et al., 2018; Gibson et al., 2012; Giles et al., 2002; Giles et al., 2004). Regardless of which  
102 interpretation is correct, by 1790 Ma lithospheric extension and thinning were well underway, and northern  
103 Australia was subjected to widespread intracontinental rifting, normal faulting and half-graben formation  
104 accompanied at deeper crustal levels by elevated heat flow, low pressure-high temperature metamorphism  
105 and bimodal magmatic intrusion (Betts et al., 2006; Gibson et al., 2012; Gibson et al., 2008; Holcombe et al.,  
106 1991; O'Dea et al., 1997a; Pearson et al., 1991). Lithospheric extension during this phase of basin formation  
107 produced mainly northwest-oriented normal faults and half-graben and continued through until ca. 1740  
108 Ma when backarc extension and rifting in the Mount Isa region and neighbouring McArthur Basin (Fig. 1a)  
109 temporarily ceased and gave way to an episode of thermal subsidence accompanied by the deposition of  
110 shallow marine quartzite and carbonate rocks (Gibson et al., 2012; Jackson et al., 2000; O'Dea et al., 1997b).

111 The Leichhardt Superbasin concluded in a period of renewed tectonic instability variously attributed to  
112 onset of a 1730–1710 Ma orogenic event (Blaikie et al., 2017) or a renewal in fault-block rotation and tilting  
113 (Gibson et al., 2012; Gibson et al., 2008). Either way, uplift and erosion accompanying this event resulted  
114 in the formation of a deeply incised and regionally extensive angular unconformity above which  
115 conglomerates and redbeds of the Bigie Formation were deposited (Fig. 3). Their deposition marks the start  
116 of the 1730–1640 Ma Calvert Superbasin in the Mount Isa region (Figs. 2 & 3) and corresponds to a  
117 resumption in backarc extension, bimodal magmatism and rift-related sedimentation across northern  
118 Australia (Gibson et al., 2016; Jackson et al., 2000; Southgate et al., 2000a). Both NW-SE and NE-SW  
119 extensional directions have been proposed for the Calvert Superbasin (Fig. 3) and questions remain about  
120 the primary orientation of half-graben hosting the bulk of basin fill. In the McArthur Basin, this includes  
121 basaltic rocks of the 1730–1720 Ma Peters Creek Volcanics and Top Rocky Rhyolite (Page et al.,  
122 2000; Rawlings et al., 2008) whereas farther afield on the Lawn Hill Platform (Fig. 1a), the Calvert  
123 Superbasin hosts basalts of the 1710–1705 Ma Fiery Creek Volcanics (Fig. 3) and fluviatile-shallow marine  
124 sediments of the 1700–1690 Ma Surprise Creek Formation (Big and Prize supersequences; Southgate et al.,  
125 2000). At about the same time that these rocks were being laid down across the Lawn Hill Platform, water  
126 depths began to substantially increase farther east so that by 1690 Ma basaltic magmas were being extruded  
127 and/or intruded into a deep marine basin filled with turbidites (Black et al., 1998; Foster and Austin,  
128 2008; Gibson et al., 2018; Gibson et al., 2012; Giles et al., 2002; Glikson et al., 1976; Neumann et al.,  
129 2009; Rubenach et al., 2008; Scott et al., 2000; Withnall, 1985). Basaltic magmatism continued through to  
130 ca. 1655 Ma in the east by which time the Leichhardt Superbasin and lower parts of the Calvert Superbasin  
131 west of the Leichhardt River Fault Trough (Fig. 1a) had been intruded by 1680–1670 Ma A-type granites

132 (Sybella Granite)(Neumann et al., 2006) and partially unroofed on top-to-the-northeast extensional shear  
133 zones (Gibson et al., 2008).

134 With the conclusion of bimodal magmatism at 1655 Ma, if not earlier at 1670 Ma in the west, the Calvert  
135 Superbasin transitioned from backarc basin to passive rifted continental margin (Baker et al., 2010;Gibson  
136 et al., 2018;Gibson et al., 2012;Neumann et al., 2009) and began to cool and subside, precipitating a marine  
137 transgression during the course of which the North Australian Craton was buried beneath a post-rift  
138 sequence (Gun-Loretta supersequences; Fig. 3) of thin-bedded turbidites, carbonaceous shales, black  
139 dolomitic siltstones and carbonate rocks that extended westwards as far as the McArthur Basin (McArthur  
140 Group; Figs. 1 & 3) and Lawn Hill Platform (Betts et al., 2016;Betts et al., 2006;Gibson et al., 2012;Gibson  
141 et al., 2017;Southgate et al., 2013;Withnall and Hutton, 2013). Passive margin conditions persisted until  
142 ca. 1650 Ma by which time northern Australia was subjected to crustal shortening and a further episode of  
143 basin inversion (Fig. 3) that lasted until at least 1640 Ma (Riversleigh Tectonic Event) and brought  
144 sedimentation in the Calvert Superbasin to a close (Gibson et al., 2018;Gibson et al., 2017;Hinman,  
145 1995;Withnall and Hutton, 2013).

146 Thereafter, the tectonic environment fundamentally changed and crustal extension resumed in a north-south  
147 direction (Fig. 3), giving rise to the 1640–1575 Ma Isa Superbasin (Fig. 2) and deposition of a further 6-8  
148 km of turbiditic sandstones, carbonaceous shales, and dolomitic siltstones (River and Term  
149 Supersequences) in fault-bounded basins, predominantly oriented ENE-WSW (Bradshaw et al.,  
150 2000;Bradshaw et al., 2018;Gibson et al., 2020;Gorton and Troup, 2018). Despite the resumption in crustal  
151 extension, basaltic rocks are absent and, save for a few tuff beds and rare 1620 Ma rhyolite sills, there was  
152 no corresponding resurgence in felsic magmatism until after crustal shortening had largely concluded at ca.  
153 1590-1580 Ma, some 50–60 Ma later (Black and McCulloch, 1990;Gibson et al., 2018;Withnall and Hutton,  
154 2013). The absence of any significant magmatism is in stark contrast to the two older superbasins, leading  
155 some researchers to conclude that the Isa Superbasin represents a sag basin, albeit one periodically  
156 punctuated by crustal extension (Betts et al., 2003;Betts et al., 2006), whereas others have argued for  
157 deposition in a foreland setting (McConachie and Dunster, 1996), pull-apart basin (Scott et al., 1998;Scott  
158 et al., 2000;Southgate et al., 2000a) or syn-orogenic basin in which extension was on-going and facilitated  
159 by orogen-parallel strike-slip faulting and lateral extrusion of continental crust (Gibson et al., 2020;Gibson  
160 et al., 2017). This episode of orogenesis concluded at ca. 1590 Ma (Gibson et al., 2020) or possibly as late  
161 as 1580 Ma (Pourteau et al., 2018) before being followed by further crustal extension and successive  
162 episodes of pluton-enhanced low pressure-high temperature metamorphism at 1560–1540 Ma and  
163 1520–1490 Ma (Duncan et al., 2011;Foster and Rubenach, 2006;Rubenach et al., 2008). Granitic rocks  
164 associated with this late metamorphism have both A- and S-type compositions and are mainly to be found  
165 in the east where they are demonstrably of post-tectonic origin, truncating and cutting across folds and axial  
166 plane fabrics produced during the Isan Orogeny (Foster and Austin, 2008;Giles et al., 2006;Page and Sun,  
167 1998;Pollard and McNaughton, 1997;Pollard et al., 1998;Withnall and Hutton, 2013).

168 Granite magmatism concluded in the east at ca. 1500–1490 Ma to be followed by further uplift and erosion  
169 across the region before the older sequences were successively buried beneath younger cover rocks of the  
170 Mesoproterozoic South Nicholson, Cambrian Georgina and Mesozoic Carpentaria basins (Sweet, 2017).  
171 Remnants of these three younger basins are still widely preserved across the Lawn Hill Platform, extending  
172 westwards across the Queensland border into the Northern Territory (Fig. 1a) where the South Nicholson  
173 Basin is thickest and occupies several different depocentres, including the Carrara Sub-basin (Fig. 4) for  
174 which a large volume of high quality seismic reflection data has recently become available (eCat:  
175 <http://pid.geoscience.gov.au/dataset/ga/69674>). Although originally acquired as part of a larger study on  
176 the South Nicholson Basin (Carr et al., 2019), these data also serve as a window on the structural  
177 architecture of the older underlying basinal sequences, and it is to this that we now turn.

### 3 Seismic record of Paleo–Mesoproterozoic basin formation and inversion in northern Australia

Survey lines for seismic reflection data acquired across the Lawn Hill Platform and already in the public domain are shown in Figure 5. Most of these are legacy lines dating back to the late 1980s and early 1990s (Burketown Survey, Comalco)(McConachie et al., 1993) and for which reprocessed data became available in 2014 (Armour Energy). Other lines (Fig. 6a & 6b) were acquired by the minerals industry (Teck Resources, 2011) or minerals industry in collaboration with state and federal Governments (Zinifex, Geological Survey of Queensland and Geoscience Australia, 2006), interpretations of which can be found in several publications and Government records (Bradshaw et al., 2018;Bradshaw and Scott, 1999;Gibson et al., 2017;Gibson et al., 2016;Krassay et al., 2000b;Scott et al., 1998;Southgate et al., 2000b). Results and interpretations of the more recent 2017 South Nicholson Basin survey (Fig. 4) were published jointly by Geoscience Australia and the geological surveys of Queensland and the Northern Territory (Carr et al., 2019) although their interpretation of geology beneath the Carrara Sub-basin (Fig. 4) is not exactly the same as the one presented here, in part owing to uncertainties in extrapolating stratigraphy from existing seismic lines into areas of little or no outcrop or exploratory drilling. The nearest exposures of older rocks are to be found in the Carrara Range immediately north of seismic line 17GA–SN1 (Fig. 4) where a few isolated outcrops of  $\geq 1850$  Ma basement schist (Kositcin and Carson, 2019) are overlain by an equally poorly exposed sequence (Carrara Range Group) of sandstones and highly altered basaltic rocks (Mitchiebo Volcanics) long regarded as correlatives of the 1780-1775 Ma Seigal Volcanics in the southern McArthur Basin (Ahmad and Munson, 2013;Rawlings et al., 2008;Sweet, 1984) and Eastern Creek Volcanics in the Leichhardt Superbasin (Fig. 3). The Carrara Range Group has been extensively intruded by the 1725 Ma Top Rocky Rhyolite (Jackson et al., 2000;Page et al., 2000) and is unconformably overlain by sedimentary rocks of equivalent age to the Isa Superbasin (Ahmad and Munson, 2013;Rawlings et al., 2008;Sweet, 1984).

In a further departure from previously published interpretations of existing seismic data (Gibson et al., 2017), the Calvert and Isa superbasins are both thought here to encompass discrete syn- and post-inversion sedimentary fractions (Fig. 3). These broadly conform with the sedimentary units or supersequences previously identified at the top of each superbasin (Bradshaw et al., 2000;Bradshaw et al., 2018;Domagala et al., 2000;Krassay et al., 2000a;Krassay et al., 2000b;Southgate et al., 2000a) and have an important bearing on basin evolution, and more particularly on the timing and duration of the basin inversion events that brought successive basin cycles to a close. These and other differences with previously published interpretations can be illustrated with a few well-chosen survey lines and there is no need to include interpretations of the full seismic dataset. All lines chosen here are composite and make for two orthogonal but not completely continuous transects across the Lawn Hill Platform, Carrara Range and neighbouring Carrara Sub-basin (Figs. 4 & 5). For an alternative and slightly different interpretation of these and other lines in the dataset, the reader is referred to Bradshaw and Scott (2009), Bradshaw et al. (2018) and Carr et al. (2019).

#### **3.1 North-south seismic transect across Lawn Hill Platform**

This composite transect is made up of several segments (Figs. 6a & 6b) oriented at high angles to the dominant ENE trend of the Isa Superbasin (Fig. 5). Collectively, these segments image a variably inverted southward-thickening sedimentary wedge disrupted by north-dipping faults and bounded at its top and bottom by major unconformity surfaces. Limited outcrop across the Lawn Hill Platform and ties to cross lines for which oil well stratigraphic data are available (Figs. 5 & 7) would further suggest that the greater part of this wedge comprises rocks of the Calvert and Isa superbasins (Bradshaw et al., 2000;Bradshaw and Scott, 1999;Gorton and Troup, 2018;Scott et al., 1998;Southgate et al., 2000a) although the former is missing its full complement of sedimentary units, having lost the Gun Supersequence and a significant

223 amount of the underlying syn-rift package to erosion so that the Loretta Supersequence now rests directly  
224 on a severely truncated Prize Supersequence (Fig. 6a). The Loretta Supersequence is itself truncated  
225 beneath the River Supersequence and thins northward through onlap onto what remains of the underlying  
226 Prize Supersequence (Fig. 6a). For this part of the Lawn Hill Platform, as much as 1700m of sedimentary  
227 section is estimated to have been removed by erosion from beneath the River Supersequence (Bradshaw et  
228 al., 2000), the greater part of which may have been redeposited farther south in the Leichhardt River Fault  
229 Trough (Fig. 1a) where there was a commensurate influx of quartz sand at or before 1640 Ma (Southgate  
230 et al., 2000b) during the closing stages of the Calvert Superbasin (Gibson et al., 2017). Basin inversion and  
231 an increase in tectonic activity during and subsequent to deposition of the Loretta Supersequence have been  
232 invoked as the most likely cause of this erosion (Bradshaw et al., 2000;Gibson et al., 2020;Gibson et al.,  
233 2017;Scott et al., 1998), consistent with the observation (Fig. 6a) that this unit is bounded top and bottom  
234 by angular unconformities and was laid down at a time of profound change as the depositional environment  
235 increasingly began to favour siliciclastic over carbonate sedimentation (Southgate et al., 2000b). Basin  
236 inversion at this time is further supported by an increase in redeposited carbonate rocks towards the top of  
237 this same supersequence (Southgate et al., 2000b) which, in turn, pass upwards into coarse sandstones and  
238 conglomerate (Shady Bore Quartzite), marking not only the base of the unconformably overlying River  
239 Supersequence but the start of the Isa Superbasin (Gibson et al., 2017). Similar unconformities have been  
240 reported in sequences of comparable age from the southern McArthur Basin (Kunzmann et al.,  
241 2019;Rawlings et al., 2008), indicating that this phase of basin inversion, uplift and erosion is more widely  
242 developed across northern Australia and is not confined to the Lawn Hill Platform. Conversely, even though  
243 rocks of equivalent age to the Leichhardt Superbasin occur widely across the McArthur Basin (Tawallah  
244 Group; Fig. 3) as well as farther south in the Leichhardt River Fault Trough (Fig. 1a), they are either missing  
245 from the seismic sections investigated here (Figs. 6a & 6b) or reduced to a thin layer sandwiched between  
246 basement and the overlying younger basins (cf Scott et al., 1998). Seismic reflections below the level of the  
247 Prize Supersequence are too poorly resolved to be confident that the rocks in question belong to one or the  
248 other of the two superbasins.

249 In marked contrast, all five supersequences of the Isa Superbasin (Fig. 3) are well imaged along Comalco  
250 line 91Bn33–91Bn28, attaining a maximum thickness of 5–6 km (Fig. 6a). Basin architecture along this  
251 particular line was first described in detail by Bradshaw et al. (2000) and their interpretation is not dissimilar  
252 to the one presented here. More specifically, as in Bradshaw et al. (2000), several inverted normal faults  
253 are recognised into which both the River and Term supersequences manifestly thicken (Fig. 6a). Normal  
254 faults of this age dip northward and even though some disrupt and offset sedimentary units in the underlying  
255 Calvert Superbasin (Loretta and Prize supersequences), there is no reason to conclude that any of these  
256 structures ever served as growth faults during deposition of the older sedimentary basin. Rather, these north-  
257 dipping faults cut across and postdate stratigraphy in the Calvert Superbasin, and first became active during  
258 deposition of the Isa Superbasin. They include the ENE-striking Bluewater and Tin Tank faults (Bradshaw  
259 et al., 2018; Pursuit Minerals, 2017), both of which dip to the north and were reactivated in the opposite  
260 sense during basin inversion (Fig. 6a). The more steeply-dipping Boga Fault (Pursuit Minerals, 2017) may  
261 similarly have been reactivated at this time but does not share the same dip or strike as the other two  
262 structures. It intersects the seismic section at nearly 90° and has a northwest strike more in keeping with  
263 other faults of Calvert-age across the region (e.g. Riversleigh Fault; Fig. 5). Moreover, unlike the Bluewater  
264 and Tin Tank faults, this structure is associated with a footwall shortcut thrust that not only accommodated  
265 a significant amount of strain during basin inversion but shares the same geometry as a similar structure  
266 developed in the footwall of the equally steeply-dipping Riversleigh Fault farther south (Fig. 6a).  
267 Importantly, neither this footwall thrust nor any of the reactivated normal faults have effected displacements  
268 large enough so as to completely disrupt stratigraphy. Instead, stratigraphy continues southward into the  
269 hangingwall of the Tin Tank Fault (Fig. 6a) where the Calvert and Isa superbasins have been spectacularly

270 deformed into a km-scale, south-verging antiformal fold (Punjab Structure). The River and Term  
271 supersequences attain maximum stratigraphic thickness in the core of this fold which is both strikingly  
272 asymmetric in character and by far the most obvious inversion structure developed along this particular  
273 segment of the north-south transect (Fig. 6a).

274 Conversely, through a combination of onlap and truncation, the Lawn and Wide supersequences both lose  
275 thickness over the crest of this same antiformal fold (Fig. 6a). Despite the loss of sedimentary record, and  
276 even more obvious truncation at the base of the overlying Mesozoic cover rocks (Fig. 6a), this thinning  
277 appears to be an original depositional feature with neither sedimentary unit ever having maintained constant  
278 stratigraphic thickness across the fold. Instead, their sedimentary thickness was strongly influenced by the  
279 presence of this structure. It follows that the Punjab Structure either already existed by the time the Lawn  
280 and Wide supersequences were deposited or the fold was actively growing during the course of their  
281 deposition. Irrespective of which interpretation is correct, these two units cannot be part of the syn-  
282 extensional growth package. Rather, extension in the Isa Superbasin had already come to a close before  
283 sedimentation ceased, and both units more rightly belong to the post-rift or syn-inversion fraction of basin  
284 fill. A similar conclusion was reached by Gibson et al (2017) for the Lawn and Wide supersequences  
285 exposed farther south along seismic line 06GA-M2 in the Century region (see below). Basin architecture  
286 in these two regions shares many similarities, not least of which is a folded and locally inverted basin fill  
287 which, in the Century region, is known to host a world class Pb-Zn mineral deposit (Southgate et al.,  
288 2000a; Southgate et al., 2006). Onlap of the River Supersequence onto older folded units in the cores of the  
289 doubly-plunging Mount Caroline and Ploughed Mountain folds (Figs. 1b & 6b) would further suggest that  
290 this was not the only episode of basin inversion to have affected the rocks of the Lawn Hill Platform.  
291 However, as elsewhere across northern Australia, the existence of the older deformational event has largely  
292 gone unrecognised owing to extensive overprinting during the 1620–1580 Ma Isa Orogeny and at least one  
293 additional shortening event that postdates the Isa Orogeny and folded all units up to and including the South  
294 Nicholson Basin (Fig. 6a). Doubly-plunging periclinal folds like Ploughed Mountain and Mount Caroline  
295 (Figs. 1b & 6b) may similarly be an expression of this younger event although, as already mentioned, they  
296 more likely first came into existence during the earlier basin inversion event and were subsequently  
297 reactivated and/or tightened during later deformation.

### 298 **3.2 West-east seismic transect through the Calvert and Isa superbasins**

299 As with the north-south transect, seismic sections oriented west-east or northeast-southwest are dominated  
300 by rocks of the Calvert and Isa superbasins and share the same wedge-like geometry (Fig. 7a & 7b). This  
301 wedge-like geometry is particularly well illustrated in composite section 89Bn07–89Bn03–89Bn06 and  
302 shows the Isa Superbasin thickening from east to west with the main sedimentary depocentre located  
303 towards the southwest as might be expected in a seismic section oriented parallel or subparallel to basin  
304 strike. Absent or difficult to recognise in either this section or 90Bn10 (Fig. 7b) are structures that might  
305 have unequivocally served as growth faults during development of the Isa Superbasin. Normal faults of this  
306 age dip predominantly northward (Fig. 6a) and as such are anticipated to have shallow-dipping or sub-  
307 horizontal traces in west-east oriented seismic sections but still cut up-section all the way to the Term  
308 Supersequence. Few structures with the requisite shallow dips have been identified in either section, and  
309 the only evidence of structural control on basin fill occurs at deeper levels in the Calvert Superbasin where  
310 the Loretta and Prize supersequences both thicken into northeast-dipping structures (Fig. 7b). Although  
311 locally disrupted by later sub-vertical faults, these structures demonstrably served as growth faults during  
312 deposition of the Calvert Superbasin and typically cut up-section no farther than the Loretta Supersequence  
313 (Fig. 7b). However, like the Riversleigh Fault (Fig. 8a) and other faults sharing the same northwest trend  
314 on the Lawn Hill Platform, these structures were subsequently reactivated in an oblique sense and continued

315 to act as growth faults during deposition of the younger River and lowermost Term supersequences (Fig.  
316 8a).

317 Following deposition of the River and lowermost Term supersequences, extension and normal faulting  
318 across the Lawn Hill Platform ceased and the syn-rift fraction of basin fill was buried beneath a post-rift  
319 blanket of near constant thickness that comprises the rest of the Term Supersequence (Figs. 7a & 7b). This  
320 was superseded, in turn, by deposition of the Lawn, Wide and Doom supersequences which, together, make  
321 up the syn-inversion package and conspicuously thin over the crest of folds developed in the hangingwalls  
322 of inverted normal faults such as the Tin Tank and Riversleigh structures (Figs. 6a & 8a). Thinning of the  
323 younger stratigraphic units across the crests of antiformal folds is no less conspicuous in the west-east  
324 oriented seismic sections shown here and is particularly evident where the underlying syn-rift sequence  
325 attains maximum thickness and has undergone the greatest amount of inversion-related uplift (Figs. 7a &  
326 7b). Such relationships are not unexpected and conform to theoretical expectations for inverted sedimentary  
327 basins (Cooper et al., 1989). They also lend support to the idea that basin inversion, and deformation more  
328 generally, had already commenced across the Lawn Hill Platform before sedimentation in the Isa  
329 Superbasin had come to a close (Gibson et al., 2017).

330 Conversely, the few large faults cutting upwards through these younger stratigraphic units from deeper  
331 levels in the Isa or Calvert superbasins are too steeply dipping to be reactivated normal faults or inversion-  
332 related structures and more likely represent strike-slip faults. Their age is not well constrained although  
333 some cut up-section as far as the South Nicholson Basin and evidently formed late. Others terminate at  
334 deeper stratigraphic levels and may be more like the Riversleigh Fault (Fig. 8a) which was reactivated in a  
335 strike-slip sense during and subsequent to the onset of north-south extension and concomitant deposition  
336 of the River and Term supersequences (Gibson et al., 2017).

### 337 **3.3 Basin inversion west of the Lawn Hill Platform**

338 Seismic reflection data collected west of the Lawn Hill Platform with a view to better understanding the  
339 mineral and hydrocarbon potential of the poorly exposed Mesoproterozoic South Nicholson Basin, and  
340 Carrara Sub-basin in particular (Fig. 4), have already been interpreted and published in their entirety (Carr  
341 et al., 2019), and this paper is only concerned with parts of the dataset that may be used to shed further light  
342 on basin architecture in the underlying older sequences. Especially pertinent in this regard are the  
343 constraints imposed by the eastern half of seismic line 17GA–SN1 (Fig. 8b) which joins onto the existing  
344 Century line (06GA–M2) just west of the Riversleigh Fault (Figs. 5 & 8a). As such, these two lines make  
345 for a single continuous and greatly expanded west-east transect through this part of northern Australia and  
346 might be expected to share a common older geology and basin architecture (Fig. 8b). An interpretation of  
347 these two lines is presented in Figures 8a – 8c and would appear to confirm that this is indeed the case for  
348 the younger post-rift and syn-inversion fractions of basin fill in the Isa Superbasin. These two fractions not  
349 only continue without break from one seismic line into the other but can be traced westwards beneath the  
350 Carrara Sub-basin for 10s of kilometres before eventually thinning over a basement high located just south  
351 of the Carrara Range (Fig. 4) where seismic lines 17GA–SN1 and SN2 intersect (see also Carr et al., 2019).  
352 This basement high developed in the hangingwall of a major south- or southeast-dipping fault or fault zone  
353 (Little Range Fault Zone) but owing to the west-east orientation of the seismic profile (Fig. 4), this structure  
354 and its hangingwall sequences are imaged in oblique section and thus dip far less steeply than in other  
355 sections oriented at higher angles to fault strike (e.g. 17GA-SN2 and 17GA-SN4). Basement rocks, along  
356 with the rest of the hangingwall sequence, have nevertheless been clearly inverted and take the form of a  
357 broad arch or subdued fold in the seismic image (Fig. 8b). No less importantly, from the thinning of younger  
358 sedimentary units onto the eastern flank of this fold (Fig. 8b), it may be further deduced that basin inversion,  
359 as in the Punjaub Structure, was already underway before the last of the Isa Superbasin had been deposited.



360 Thinning of the younger stratigraphic units aside, it is equally evident from the seismic data that the  
361 hangingwall of the Little Range Fault Zone comprises a less than complete sedimentary record (Fig. 8b).  
362 The syn-rift fraction of basin fill (River and lowermost Term supersequences) and any unit that might be  
363 reliably identified as part of the Calvert Superbasin are missing and do not appear to extend any farther  
364 west than the Riversleigh Fault (Figs. 8a & 8b). Particularly conspicuous by its absence is the Loretta  
365 Supersequence whose transparent to weakly reflective character in seismic sections (Bradshaw et al.,  
366 2000;Southgate et al., 2000a) is usually enough to distinguish it from other stratigraphic units in the Calvert  
367 and Isa Superbasins (e.g. Figs. 6 –7). Either this and the other missing sedimentary units were never  
368 deposited west of the Riversleigh Fault or, as elsewhere across the region, these rocks have been removed  
369 by erosion so that younger elements of the Isa Superbasin have come to directly overlie older rocks thought  
370 (Gibson et al., 2017) to form part of the Leichhardt Superbasin (Figs. 8a & 8b). Stratigraphy in this older  
371 basin is variably truncated beneath rocks of the overlying Isa Superbasin and, like them, can be traced  
372 westwards for some distance towards the Little Range Fault Zone and its basement high, and over the top  
373 of which the older rocks almost reach the surface (Fig. 8b). Nowhere, however, along the seismic line are  
374 the older rocks actually exposed. A thin veneer of Cambrian and/or Mesozoic sediments (Georgina and  
375 Carpentaria basins) always intervenes although rocks long thought (Ahmad and Munson, 2013;Rawlings  
376 et al., 2008) to be correlatives of the Leichhardt Superbasin (Fig. 3) are exposed north of the seismic line  
377 in the Carrara Range (Carrara Range Group: Fig. 4). Moreover, these rocks have since been shown to have  
378 the same age as the Leichhardt Superbasin based on strikingly similar detrital zircon populations (Kositcin  
379 and Carson, 2019). They also rest unconformably on  $\geq 1840$  Ma psammopelitic schists which not only  
380 represent basement to the Carrara Range Group in this region (Ahmad and Munson, 2013;Rawlings et al.,  
381 2008) but likely serve as a good proxy for unexposed basement along the seismic line a short distance to  
382 the south.

383 West of the Little Range Fault Zone is a second, even larger uplifted basement block or horst bounded on  
384 its eastern side by a steeply-dipping fault and inverted sedimentary basin (Fig. 8c) filled almost entirely by  
385 rocks of the Isa Superbasin. Basin fill is up to 10 km-thick and strikingly similar in both volume and  
386 geometry to the correlative sequence exposed in the hangingwall of the Riversleigh Fault farther east (Fig.  
387 8a). As with the latter, this includes the full complement of post-rift and syn-inversion sedimentary units  
388 (Lawn, Wide and Doom supersequences) as well as a thicker syn-rift package of more strongly reflective  
389 rocks interpreted here (Fig. 8c) to be made up of the River and Term supersequences. The River  
390 Supersequence is particularly well represented, thickening into the Old Man's Fault (informal name) and  
391 characteristically exhibiting a wedge-like geometry that thins eastwards through overlap onto the adjacent  
392 basement high and its cap of Leichhardt Superbasin (Fig. 8c). Its contact with the underlying older rocks  
393 just west of the Little Range Fault Zone is an angular unconformity beneath which the Leichhardt  
394 Superbasin is abruptly truncated or lost altogether so that the Isa Superbasin rests directly on the underlying  
395 basement (Fig. 8c). Significantly, this same angular relationship has been observed in outcrop in the Carrara  
396 Range (Sweet, 1984) where rocks of the McNamara Group (Isa Superbasin) directly overlie the Carrara  
397 Range Group (Leichhardt Superbasin equivalents). It is thus not unreasonable to conclude that the River  
398 Supersequence was deposited on an already uplifted and eroded surface that cuts downward ever more  
399 deeply in a southerly or east to west direction so as to expose progressively older elements of the regional  
400 stratigraphy in and around the Carrara Range. Moreover, even though the bulk of this uplift and erosion  
401 likely occurred during the 1650–1640 Riversleigh Tectonic Event immediately prior to deposition of the  
402 River Supersequence, the possibility that some of it dates from an even older 1730 Ma episode of  
403 deformation better known from the McArthur Basin as the mid-Tawallah Compressional Event (Ahmad  
404 and Munson, 2013) cannot be excluded. Notwithstanding such uncertainties, basement and its bounding  
405 faults clearly played an important role in controlling basin architecture and continued to be active long after  
406 deposition of the Isa Superbasin had concluded as both the South Nicholson and Georgina basins similarly

407 thin across them (Fig. 8c). Equally notable in this context is an obvious reversal in basin and fault polarity  
408 on either side of the larger basement horst block (Fig. 8b).

### 409 **3.4 North-south seismic sections orthogonal to 17GA-SN1**

410 As a further check on basin geometry and structural architecture to the west of the Lawn Hill Platform, two  
411 sections (17GA-SN2 and 17GA-SN4) were selected for interpretation in a direction at a high angle or  
412 orthogonal to 17GA-SN1 (Figs. 9a & 9b). With its NW-SE orientation, seismic line 17GA-SN2 cuts across  
413 many of the same structures imaged in 17GA-SN1, most notably at least one crustal-scale south- or  
414 southeast-dipping shear zone or fault system that extends downward into the lower crust and possibly as  
415 far as the MOHO (Figs. 8b & 9a). This shear zone is several hundred metres wide and is likely the same  
416 reactivated basement structure identified as the Little Range Fault Zone along line 17GA-SN1; it has  
417 variably deformed rocks of the Leichhardt and Isa superbasins in its hangingwall (Fig. 9a) and appears to  
418 have served as a thrust system during basin inversion, effecting upward displacement not only of the former  
419 but the underlying basement rocks. The most obvious difference between lines 17GA-SN1 and 17GA-SN2  
420 is the thick wedge-like basinal sequence imaged down to 7.0 seconds TWT in the hangingwall of this same  
421 shear zone (Fig. 9a). This basinal sequence lies below the interpreted base of the Leichhardt Superbasin in  
422 line 17GA-SN1 (Fig. 8b) and either represents an entirely separate older volcanic/sedimentary package or  
423 a continuation of the Leichhardt Superbasin downward to much greater depths than is immediately apparent  
424 in the west-east oriented seismic section. In the absence of independent information, it is not possible to  
425 discriminate between these two possibilities except to say that the same package is evidently present in line  
426 17GA-SN1 and corresponds to a zone of non-reflective crust which at a depth of 10 kilometres or more  
427 seems much too deep for the Leichhardt Superbasin (Fig. 9a) and shares none of the higher amplitude  
428 reflectors common to other seismic lines through this basin elsewhere in the Mount Isa region (e.g.  
429 06GA-M3; Gibson et al., 2016). Several other low-angle faults imaged in lines 17GA-SN1 and 17GA-SN2  
430 also root downward into this zone (Figs. 8b & 9a) although neither they nor the surfaces bounding the older  
431 sedimentary package are particularly conspicuous or maintain their individual character at depth. Rather,  
432 all of these faults and surfaces merge downward into one seismically bland and homogenised region of  
433 middle crust more in keeping with expectations for metamorphic basement than the Leichhardt Superbasin.  
434 Moreover, because line 17GA-SN1 is probably more closely aligned with lithological strike in the older  
435 sedimentary package and its bounding surfaces, their apparent dip in this particular seismic section is close  
436 to zero, resulting in surfaces whose traces are subhorizontal and parallel to each other. Only along line  
437 17GA-SN2 is the northern dip of this older seismic package discernible.

438 As with the other two seismic lines across the South Nicholson Basin, 17GA-SN4 has imaged a basement  
439 block overlain by a southward-thickening wedge of sedimentary rocks mainly belonging to the Isa  
440 Superbasin but beneath which there is a variably truncated and faulted older sequence. This older sequence  
441 rests directly on basement and likely incorporates correlatives of the Leichhardt Superbasin (Fig. 9b).  
442 Seemingly missing again is the Calvert Superbasin and its place has been taken up by a package of rocks  
443 (Fig. 9b) whose seismic character (short, high amplitude reflectors) is a better fit for the River and/or Term  
444 Supersequence as opposed to the Loretta or Prize supersequences. Lying above this package are several  
445 sedimentary units identified elsewhere in this paper as belonging to the post-rift and syn-inversion fractions  
446 of basin fill in the Isa Superbasin. They, in turn, are overlain by younger sediments of the South Nicholson  
447 and Georgina basins although the latter is very thin and represents no more than a veneer over the underlying  
448 rocks (Fig. 9b).

449 Importantly, essentially the same stratigraphic package can be identified north of the seismically imaged  
450 basement block, except that all sedimentary units, including those making up the South Nicholson Basin,  
451 are appreciably thicker and have a different geometry, pointing to deposition in a separate sub-basin to the

452 Carrara Sub-basin (Fig. 9b). In keeping with this interpretation, the two depocentres are separated by a  
453 major fault which dips steeply south and is likely an along-strike continuation of the same south-dipping  
454 fault system (Little Range Fault Zone) imaged farther west along seismic lines 17GA-SN1 and SN2. As  
455 with the other two structures, this fault played an equally important role in basin formation and was  
456 reactivated on more than one occasion because sedimentary units in its hangingwall, up to and including  
457 the South Nicholson Basin, have all been inverted whereas older rocks in its footwall are cut by this  
458 basement fault and terminate abruptly against it. This includes rocks of the River and/or Term  
459 supersequences which were deposited on an older and already folded older sequence taken here to be  
460 Paleoproterozoic Carrara Range Group (Fig. 9b) and thus part of the Leichhardt Superbasin (Fig. 3). No  
461 less conspicuously, this older sequence thickens towards basement and its bounding fault, whereas  
462 sedimentary sequences making up the overlying South Nicholson Basin and higher levels of the Isa  
463 Superbasin (Lawn through to Doom supersequences) do the opposite; they instead thin towards this  
464 basement high and likely overlapped the latter at the time these rocks were being deposited. The seismic  
465 images are consistent with such an interpretation, particularly for the higher level sedimentary units (Fig.  
466 9b), which still show significant amounts of thinning over the adjacent basement high despite successive  
467 episodes of fault reactivation. Sedimentation, paired to uplift and erosion has been observed before in the  
468 Paleo-Mesoproterozoic basins of Northern Australia and usually attributed to repeated episodes of rift-sag  
469 (Betts et al., 2016; Betts et al., 2003; Betts et al., 2006; O'Dea et al., 1997b) or strike-slip faulting along basin-  
470 bounding structures (Scott et al., 1998; Southgate et al., 2000b). Basin inversion with a few notable  
471 exceptions (Blaikie et al., 2017; Broadbent et al., 1998; Gibson et al., 2017) was largely treated as a late or  
472 secondary process and thus incidental to the formation of Pb–Zn mineral deposits. Interpreted seismic data  
473 presented in this paper would suggest otherwise and that basin inversion as a process had a far greater  
474 impact on basin history and mineralisation than has hitherto been recognised.

## 475 **4 Discussion**

### 476 **4.1 Basin inversion structures: timing and distribution**

477 Inverted extensional basins and their structural architecture have been widely investigated and described  
478 following numerous field studies combined with the results of numerical modelling and sandbox  
479 experiments (Cooper et al., 1989; Hayward and Graham, 1989; McClay et al., 2002; McClay and White,  
480 1995; Turner and Williams, 2004). Emphasised in most of these studies is the strongly asymmetric nature  
481 of the pre-existing basin fill and the consequences of shortening a sedimentary sequence whose individual  
482 unit lengths are all different and increase upward from bottom to top of the section (Hayward and Graham,  
483 1989; Lowell, 1995; Turner and Williams, 2004). The net result during shortening is development of an  
484 equally asymmetric fold in the hangingwall of the original normal fault which may or may not have been  
485 reactivated during the process. This hangingwall fold is one of the most distinctive features of basin  
486 inversion and may be regarded as a diagnostic feature, particularly in cases where folding is enhanced by  
487 the reactivation of coeval antithetic structures leading to the expulsion of basin fill in opposite directions.  
488 Further enhancements of the basic inverted structure may occur where the normal fault locks up early and  
489 strain is transferred to a footwall shortcut thrust or taken up by some other structure such as a strike-slip  
490 fault (Dooley and McClay, 1997; McClay, 1995; McClay et al., 2002). These and other variations on  
491 structural architecture developed during basin inversion (Martínez et al., 2012) are illustrated in Figure 10.  
492 All examples are from inverted basins of Mesozoic or younger age but are clearly no less relevant in the  
493 case of the older basins described here from northern Australia. Footwall shortcut thrusts have been  
494 captured in several of the seismic sections but are conspicuously well developed in the footwalls of the  
495 Riversleigh (06GA–M2) and Boga structures (Figs. 8a & 6b). However, by far the most common and  
496 widely imaged structure is the hangingwall antiform (Fig. 10). Moreover, this same structural feature is  
497 evident in all sections irrespective of whether they are oriented north-south or west-east, supporting

498 suggestions made elsewhere that there has been more than one episode of basin inversion and that these  
499 were imposed on basins that were originally orthogonal to one another. As such, basin inversion affords  
500 clues to basin orientation before and after successive episodes of crustal shortening got underway and it is  
501 to this topic that we now turn.

502 The Isa Superbasin is best known from the Lawn Hill Platform (Fig. 5) and has been previously interpreted  
503 as a sag or foreland basin deformed during a subsequent north-south shortening event identified as the Isan  
504 Orogeny (Betts et al., 2003;McConachie et al., 1993;McConachie and Dunster, 1996). More recently, an  
505 extensional origin has been proposed for this same basin consistent with seismic data and general thickening  
506 of sedimentary units like the River and Term supersequences into normal faults oriented ENE-WSW  
507 (Bradshaw et al., 2018;Gorton and Troup, 2018). Antiformal closures developed in the Punjaub Structure  
508 and periclinal folds exposed just to its south at Mount Caroline and Ploughed Mountain share the same  
509 ENE-WSW trend (Fig. 1b) and likely represent basin inversion structures formed during the same north-  
510 south shortening event. However, as already pointed out, the Punjaub Structure is not a simple structure  
511 and likely underwent limited folding before or subsequent to the start of deposition in the River and Term  
512 supersequences (Gibson et al., 2020). Along with rocks of Calvert age in the core of the Punjaub Structure,  
513 these two sequences were deformed during the 1650–1640 Ma Riversleigh Tectonic Event for which a NE-  
514 SW shortening direction has been proposed (Gibson et al., 2020;Gibson et al., 2017). As such, shortening  
515 during the earlier stages of basin inversion in the Punjaub Structure would have been approximately  
516 orthogonal to strike in the Calvert Superbasin and its NW-SE basin-bounding normal faults. Seismic  
517 sections oriented parallel to this shortening direction consistently show faults of Calvert age dipping  
518 eastwards (e.g. Riversleigh Fault) and several have antiformal structures developed in their hangingwalls  
519 (Figs. 8a & 8b) in accord with expectations that basin geometry prior to inversion was highly asymmetric  
520 and had the form of a westward deepening half-graben. Westward deepening of Calvert-age extensional  
521 basins on the Lawn Hill Platform is contrary to the results of earlier geophysical modelling (Betts et al.,  
522 2004) indicating that half-graben of this age deepen southwards towards normal faults with NE orientations  
523 essentially orthogonal to what is proposed here. However, while faults with this orientation have been  
524 previously mapped (Hutton and Sweet, 1982) or have been known to exist in the subsurface for a long time  
525 (Krassay et al., 2000a;Scott et al., 1998), it is debatable that they are of Calvert age or exercised any  
526 significant control on depositional patterns during this phase of basin formation. They share the same NE  
527 to ENE strike as normal faults in the Isa Superbasin and likely belong to the same generation of structures  
528 that controlled deposition of the younger sedimentary basin. Importantly, faults of this age exhibit increased  
529 amounts of throw southwards which would have been accompanied by commensurate amounts of  
530 downward displacement in rocks of the underlying Calvert Superbasin, as captured in seismic images (Fig.  
531 6a) along line 91Bn28–91Bn33 and the northern flank of the Punjaub Structure where the Loretta and Prize  
532 supersequences, along with older elements of the Isa Superbasin, have been faulted downward by several  
533 kilometres relative to their counterparts across the crest of the fold. This is the same stepped basin geometry  
534 picked up in the results of geophysical modelling for the Lawn Hill Platform (Betts et al., 2004) and which,  
535 during later crustal shortening, would have produced south-verging folds with the same NE axial direction  
536 orientation as periclinal folds now observed at Mount Caroline and Ploughed Mountain (Fig. 1b). It further  
537 follows that the NW-SE extensional direction previously proposed for the Calvert Superbasin more likely  
538 relates to the younger Isa Superbasin and only came about because erosion across the Lawn Hill Platform  
539 during or subsequent to the Isa Orogeny removed much of the younger basin infrastructure leaving behind  
540 only the inverted and once more deeply buried rocks of the older basin.

541 West of the Lawn Hill Platform, crystalline basement lies at much shallower crustal depths and may even  
542 have been exposed during deposition of the Georgina or South Nicholson basins, forming one or more  
543 structural highs over the top of which there is a conspicuous thinning or draping of the younger cover rocks

(Fig. 9b). The older Paleoproterozoic–early Mesoproterozoic sequences are similarly notably thinner over basement in this region and the Calvert Superbasin may be entirely missing (Figs. 8b & 9b), either because it was never deposited or was removed by erosion during uplift accompanying the Riversleigh Tectonic Event. The River Supersequence consequently directly overlies a truncated and westward thinning older sequence taken here to be the Leichhardt Superbasin based on continuity with line 06GA–M2 (Fig. 8a) for which a stratigraphic interpretation has already been published. As with line 06GA–M2 (Fig. 8a), an angular unconformity separates the two sequences (see also Sweet, 1984), and the Leichhardt Superbasin had likely already been inverted before the River Supersequence was laid down. In keeping with this suggestion, the older sequence has locally been completely eroded away so that the River Supersequence rests directly on older crystalline basement (Fig. 8b). Moreover, even though a significant amount of this uplift and erosion may have been accommodated on reactivated older normal faults, the dominant structures in the seismic images are sub-vertical to steeply dipping and abruptly truncate stratigraphy not only in basement but thick basinal sequences developed in their footwalls. These footwall sequences encompass most if not all units of the Isa Superbasin (Figs. 8b & 9b), pointing to either a considerable amount of downward throw to the north on these structures or an equally significant amount of strike-slip displacement. The latter is thought more likely here consistent with the scale and abruptness of truncation and the observation that the faults overall have the character of flower-like structures (Fig. 9b). Such uncertainties aside, it seems reasonable to conclude that basement uplift on these subvertical faults occurred late as these structures displace all units in the Isa Superbasin and cut up-section all the way to the base of the Cambrian. Faults with similarly steep attitudes and character are also evident in north-south oriented seismic sections (Fig. 6) for the northern Lawn Hill Platform (e.g. 91Bn28–91Bn33) and likely belong to the same generation of strike-slip faults. Significantly, they share the same NE to ENE strike and were possibly initiated on older structures dating back to formation of the Isa Superbasin into which they root downward (Fig. 6a). Late NE-trending strike-slip faulting has recently been attributed to the onset of extensional collapse and orogen-parallel extrusion of thermally weakened crust following arc-continent or continent-continent collision between Australia and Laurentia (Gibson et al., 2020).

#### **4.2 Basin inversion and implications for Pb–Zn mineralisation**

As revealed in seismic sections oriented orthogonal to one another, basin inversion in the north Australian Paleoproterozoic–Mesoproterozoic sequences occurred on more than one occasion and gave rise to a structural architecture not unlike that recorded in basins of much younger age such as the Irish and North seas and North Atlantic petroleum province more generally. No less important in this context are the results of past and recent drilling confirming that northern Australia is prospective for oil and gas (Gorton and Troup, 2018; Jackson et al., 1986; McConachie et al., 1993), not all of which has its source in the South Nicholson or younger sedimentary basins (Glikson et al., 2006; Golding et al., 2006). Some is known to be considerably older (Jackson et al., 1986) or at least date back to the time of Pb–Zn mineralisation in the 1575 Ma Century deposit (Broadbent et al., 1998). Bituminous residues occur widely throughout this deposit (Broadbent et al., 1998) and more recent studies have shown that carbonaceous shales and dolomitic siltstones hosting the ore body (Wide Supersequence) contain exceptionally high levels of total organic carbon, along with other parts of the Isa Superbasin (Glikson et al., 2006; Gorton and Troup, 2018; Jarrett et al., 2018). However, this need not imply that the mineralising fluids were emplaced into an existing oil or gas reservoir as required by the Broadbent et al. (1998) model for ore formation. An alternative possibility is that the organic matter was already present in the host rocks from the time they were deposited and got transformed into oil and/or gas during ingress of the mineralising fluid itself (Glikson et al., 2006; Golding et al., 2006). Either way, it is difficult to avoid the conclusion that a petroleum system was in operation during or immediately prior to mineralisation. Moreover, if fluid:rock ratios were high at the time of mineralisation, much of the organic carbon would have been removed from the deposit site, leaving behind

590 bituminous residues but more importantly leading to transient increases in pore space that was subsequently  
591 filled by sulphides (Glikson et al., 2006). Stable isotope studies combined with analyses of illite crystallinity  
592 and organic reflectance would further indicate that this processes occurred under a normal thermal gradient  
593 (ca.  $24^{\circ}\text{Ckm}^{-1}$ ) and temperatures below  $200^{\circ}\text{C}$  (Glikson et al., 2006;Golding et al., 2006) and thus without  
594 the need for additional magmatic or metamorphic heating. Bimodal magmatism ceased some 60–70 Myr  
595 earlier at ca. 1655 Ma and so any related thermal anomaly would have long since decayed and been  
596 unavailable to drive either fluid flow or the mineralisation process. Instead, any extraneous heat added to  
597 the system may have come from the hydrothermal fluids themselves whose expulsion from deeper levels  
598 of the basin was more likely driven by a build-up of fluid overpressures as the twin processes of crustal  
599 shortening and basin inversion took effect.

600 Significantly, a near-identical scenario have been proposed for some carbonate-hosted Pb–Zn deposits of  
601 Mississippi Valley-type (Leach et al., 2001;Leach et al., 2010) which nearly always contain some amount  
602 of pyrobitumen or organic carbon and may similarly have formed through mixing of hydrocarbons with a  
603 hydrothermal metal-bearing fluid (Anderson, 2008;Kesler et al., 1994). Such similarities with Century and  
604 the clastic-dominated Pb–Zn deposits of northern Australia have been noted before (Huston et al., 2006)  
605 but are usually tempered by perceived differences in tectonic setting or the timing of mineralisation relative  
606 to orogenesis. A compressional foreland setting is usually advanced for the former (Leach et al., 2001)  
607 whereas the Pb–Zn deposits of northern Australia are thought to be largely syn-extensional in origin and  
608 form prior to the onset of orogenesis (Huston et al., 2006;Large et al., 2005). In the interpretation presented  
609 here, there is no discernible difference in tectonic setting between the two different deposit styles, and late  
610 Paleoproterozoic-early Mesoproterozoic Pb–Zn mineralisation at Century and elsewhere across the region  
611 was driven by basin inversion linked to orogenesis and crustal shortening (Gibson et al., 2020;Gibson et  
612 al., 2017) as originally envisaged by Broadbent et al. (1998).

613 Moreover, in view of seismic evidence for basin inversion towards the end of Calvert time (e.g. Fig. 6a),  
614 there is no reason why the Walford Creek Pb–Zn deposit (Rohrlach et al., 1998) located just to the north of  
615 Century (Fig. 1a) could not have formed under similar circumstances. Although older, and hosted by  
616 carbonate rocks of the Loretta Supersequence (Walford Dolomite), its host rocks were similarly laid down  
617 during a period of increasing tectonic instability (Riversleigh Tectonic Event). The deposit itself has also  
618 been described as being of Mississippi Valley-type (Rohrlach et al., 1998). No less importantly, fluid  
619 inclusions from this ore body are known to contain light oil (Rohrlach et al., 1998), most likely sourced and  
620 introduced ahead of mineralisation from shales rich in organic carbon (Mount Les Siltstone) in the overlying  
621 River Supersequence (Glikson et al., 2006). Thus, not only were hydrocarbons leaking from one  
622 stratigraphic unit into another in this region but there is a strong possibility that a petroleum system was  
623 present up to and possibly including the time of mineralisation. Accordingly, as at Century, the mineralising  
624 fluid may have interacted or mixed with organic carbon, making for a highly reducing environment into  
625 which more oxidised metal-bearing fluids were introduced, and doubly so if the hydrocarbon fluid was  
626 contaminated by sour gas and contained appreciable amounts of hydrogen sulphide as is often the case with  
627 Mississippi Valley-type Pb–Zn deposits (Anderson, 2008;Huston et al., 2006). On encountering this  
628 reducing environment, a number of catalysed redox reactions ensued during the course of which existing  
629 carbonate minerals were dissolved and metal sulphides precipitated in their place. Metal precipitation in  
630 other Pb–Zn deposits across the region, including Mount Isa, was likely driven by similar replacement  
631 reactions following upward transport of metalliferous fluids sourced from deeper levels of the basin. Fluids  
632 may initially have travelled up reactivated faults but on arrival at the ore formation site became trapped and  
633 migrated into their hangingwalls or footwall shortcut thrusts where they brought about dissolution of the  
634 host rock and its replacement by sulphides. This compares with current ore formation models where the  
635 mineralising fluid was introduced along basin-bounding structures active at the time of basin formation

636 (Huston et al., 2006;Large et al., 2005;McGoldrick et al., 2010;Southgate et al., 2000b) or along normal  
637 faults reactivated in the opposite sense during periods of transient crustal shortening in an overall  
638 extensional or sag setting (Betts et al., 2003;Kunzmann et al., 2019). Mineral exploration has accordingly  
639 often been directed towards the identification of structures and sedimentary sequences formed during the  
640 course of basin formation as opposed to those that may have formed during later basin inversion.

641 However, as is now evident from recent seismic interpretations of line 06GA–M2 (Gibson et al.,  
642 2017;Gibson et al., 2016), the carbonaceous rocks hosting Century belong to the syn-inversion fraction of  
643 basin fill and were deposited at a time of crustal shortening accompanying the Isan Orogeny. There is no  
644 evidence that this shortening was accompanied by reactivation of the basin-bounding structure. Instead, as  
645 with many normal faults, the Riversleigh Fault dipped too steeply to be easily reactivated and strain was  
646 taken up on a footwall shortcut thrust; it rather than the Riversleigh Fault would have served as the better  
647 fluid conduit. Interestingly, the Termite Range Fault has some of the same attributes as a footwall shortcut  
648 thrust and is widely believed (Broadbent et al., 1998;Yang and Radulescu, 2006) to have been the main  
649 fluid conduit for the Century deposit which lies either above or in a minor offshoot immediately adjacent  
650 to the master structure. No less importantly, mineralisation is transgressive with respect to stratigraphy and  
651 occurred through replacement processes (Broadbent et al., 1998), consistent with the 1575 Ma age reported  
652 for this deposit (Carr et al., 2004). This is long after the start of crustal shortening and probable concomitant  
653 expulsion of hydrocarbons to higher stratigraphic levels where they would have pooled or been trapped in  
654 structures formed during inversion. It seems further likely, if the analogy with the petroleum system has  
655 any validity, that a significant amount of this metal-bearing fluid found its way into the same type of  
656 hangingwall structures that are so prospective of oil and gas in the younger inverted basins of the North  
657 Atlantic petroleum province. If this is indeed the case, then a change in exploration strategies for sediment-  
658 hosted Pb–Zn mineralisation may be warranted where there is less focus on the identification of normal  
659 faults active at the time of basin formation towards increased targeting of potential structural traps located  
660 in either the footwalls or less proximal parts of their inverted hangingwall structures.

661 Importantly, owing to asymmetries inherited from the original basin architecture, the default position for  
662 the latter will be the same regions where basin fill attained maximum thickness and source rocks were  
663 sufficiently deeply buried to generate the requisite volumes of metalliferous fluids during basin inversion.  
664 Potential source rocks for Pb and Zn metal include the syn-rift component of basin fill which, in these  
665 regions, might be expected to include thick sequences of altered volcanic and immature sedimentary rocks  
666 as was reportedly the case for mineral deposits in the McArthur Basin and Leichhardt River Fault Trough  
667 (Cooke et al., 1998;Heinrich et al., 1995;Huston et al., 2016;Huston et al., 2006;Polito et al., 2006;Southgate  
668 et al., 2006). However, as revealed by the seismic data, substantial amounts of the Calvert and Leichhardt  
669 superbasins were removed through erosion during inversion so that neither the full complement of syn-rift  
670 rocks nor any vestige of a basin seal need be preserved in one or both basins (e.g. 17GA–SN1 and SN2).  
671 Basin seals and barriers to upward fluid flow are more likely to be found among the finer-grained  
672 carbonaceous shales and dolomitic siltstones making up the post-rift fraction of basin fill but this is the very  
673 component most susceptible to uplift and erosion during the initial stages of basin inversion. Accordingly,  
674 the optimal site for the formation and preservation of Pb–Zn mineralisation may be in basins whose inverted  
675 hangingwalls and related structures never lost all of their post-rift capping rocks and continued to evolve  
676 beneath succeeding layers of tectonically-driven sedimentation. In either event, it is difficult to avoid the  
677 conclusion that basin inversion played an important, if not critical, role in the formation of a world-class  
678 Pb–Zn mineral province in northern Australia.

#### 679 **Data Availability.**

680 Uninterpreted seismic reflection images on which this paper is based are available online from the  
681 respective Government data repositories: (Geoscience Australia eCat:

682 <http://pid.geoscience.gov.au/dataset/ga/69674>) and Queensland Geological Survey:  
683 <https://qdexdata.dnrme.qld.gov.au/QDEXDataDownloadManager/Results?type=Seismic&id=95456,95541,91004>.  
684

#### 685 **Author contributions.**

686 GMG undertook most of the seismic interpretations, compiled the figures and wrote the initial draft of the  
687 article; SE critically reviewed the seismic interpretations and initial draft of the manuscript, researched  
688 the implications of basin inversion on the petroleum system and contributed written commentary on the  
689 latter that formed the foundations of a revised and expanded discussion section. Both authors participated  
690 in a powerpoint discussion on basin inversion at GSQ in late 2019 that formed the basis for this paper.

#### 691 **Competing interests.**

692  
693 The authors declare that they have no conflict of interest.  
694

#### 695 **Acknowledgements.**

696 For the invitation and opportunity to contribute to the special anniversary volume on basin inversion we  
697 thank editors, professors Jonas Kley and Piotr Krzywiec. For detailed and comprehensive reviews that  
698 greatly improved the text we are indebted to Professor Alan Collins and Dr Karen Connors. Thanks also  
699 to Teck Resources Australia and Pursuit Minerals for permission to publish our interpretation of the  
700 Punjaub Structure. Figure 2 was produced on our behalf by Dr Ian Withnall, Geological Survey of  
701 Queensland.  
702

## 703 **5 References**

- 704 Ahmad, M., and Munson, T. J.: Chapter 18: Lawn Hill Platform, in: *Geology and mineral resources of the Northern*  
705 *Territory, Special Publication 5*, edited by: Ahmad, M., and Munson, T. J., Northern Territory Geological Survey,  
706 Darwin, 2013.
- 707 Anderson, G. M.: The mixing hypothesis and the origin of Mississippi Valley-type deposits, *Economic Geology*, 103,  
708 1683-1690, 2008.
- 709 Andrews, S. J.: Stratigraphy and depositional setting of the upper McNamara Group, Lawn Hill region, northwest  
710 Queensland, *Economic Geology*, 93, 1132-1152, 10.2113/gsecongeo.93.8.1132, 1998.
- 711 Baker, M. J., Crawford, A. J., and Withnall, I. W.: Geochemical, Sm-Nd isotopic characteristics and petrogenesis of  
712 Paleoproterozoic mafic rocks from the Georgetown Inlier, north Queensland: Implications for relationship with  
713 the Broken Hill and Mount Isa eastern succession, *Precambrian Research*, 177, 39-54, 2010.
- 714 Betts, P. G., and Lister, G. S.: Comparison of the 'strike-slip' versus the 'episodic rift-sag' models for the origin of  
715 the Isa Superbasin, *Australian Journal of Earth Sciences*, 48, 265 - 280, 2001.
- 716 Betts, P. G., Giles, D., and Lister, G. S.: Tectonic environment of shale-hosted massive sulphide Pb-Zn-Ag deposits  
717 of Proterozoic northeastern Australia, *Economic Geology*, 98, 557-576, 2003.
- 718 Betts, P. G., Giles, D., and Lister, G. S.: Aeromagnetic patterns of half-graben and basin inversion: Implications for  
719 sediment-hosted massive sulfide Pb-Zn-Ag exploration, *Journal of Structural Geology*, 26, 1137-1156,  
720 <http://dx.doi.org/10.1016/j.jsg.2003.11.020>, 2004.
- 721 Betts, P. G., and Giles, D.: The 1800-1100 Ma tectonic evolution of Australia, *Precambrian Research*, 144, 92-125,  
722 2006.
- 723 Betts, P. G., Giles, D., Mark, G., Lister, G. S., Goleby, B. R., and Ailleres, L.: Synthesis of the Proterozoic evolution of  
724 the Mount Isa inlier, *Australian Journal of Earth Sciences*, 53, 187-211, 2006.
- 725 Betts, P. G., Armit, R. J., Stewart, J., Aitken, A. R. A., Ailleres, L., Donchak, P., Hutton, L., Withnall, I., and Giles, D.:  
726 Australia and Nuna, Geological Society, London, Special Publications, 424, 47-81, 10.1144/sp424.2, 2016.



727 Bierlein, F. P., Black, L. P., Hergt, J., and Mark, G.: Evolution of pre-1.8 Ga basement rocks in the western Mt Isa  
728 Inlier, northeastern Australia--insights from Shrimp U-Pb dating and in-situ Lu-Hf analysis of zircons, *Precambrian*  
729 *Research*, 163, 159-173, 2008.

730 Bierlein, F. P., Maas, R., and Woodhead, J.: Pre-1.8 Ga tectono-magmatic evolution of the Kalkadoon–Leichhardt  
731 belt: Implications for the crustal architecture and metallogeny of the Mount Isa Inlier, northwest Queensland,  
732 Australia, *Australian Journal of Earth Sciences*, 58, 887-915, 10.1080/08120099.2011.571286, 2011.

733 Black, L. P., and McCulloch, M. T.: Isotopic evidence for the dependence of recurrent felsic magmatism on new  
734 crust formation: An example from the Georgetown region of northeastern Australia, *Geochimica et Cosmochimica*  
735 *Acta*, 54, 183-196, 1990.

736 Black, L. P., Gregory, P., Withnall, I. W., and Bain, J. H. C.: U-Pb zircon age for the Etheridge Group, Georgetown  
737 region, north Queensland: Implications for relationship with the Broken Hill and Mt Isa sequences, *Australian*  
738 *Journal of Earth Sciences*, 45, 925 - 935, 1998.

739 Blaikie, T. N., Betts, P. G., Armit, R. J., and Ailleres, L.: The ca. 1740–1710 Ma Leichhardt Event: Inversion of a  
740 continental rift and revision of the tectonic evolution of the North Australian Craton, *Precambrian Research*, 292,  
741 75-92, <http://dx.doi.org/10.1016/j.precamres.2017.02.003>, 2017.

742 Blake, D. H.: Geology of the Mount Isa inlier and environs, Queensland and Northern Territory, *BMR Bulletin*, 225,  
743 83, 1987.

744 Bradshaw, B. E., and Scott, D. J.: Integrated basin analysis of the Isa Superbasin using seismic, well-log and  
745 geopotential data: An evaluation of the economic potential of the northern Lawn Hill Platform, *Australian*  
746 *Geological Survey Organisation (now Geoscience Australia) AGSO Record 199/19 (Digital Version)*, Canberra,  
747 1999.

748 Bradshaw, B. E., Lindsay, J. F., Krassay, A. A., and Wells, A. T.: Attenuated basin-margin sequence stratigraphy of  
749 the Palaeoproterozoic Calvert and Isa superbasins: The Fickling Group, southern Murphy Inlier, Queensland,  
750 *Australian Journal of Earth Sciences*, 47, 599 - 623, 2000.

751 Bradshaw, B. E., Orr, M. L., Bailey, A. H. E., Palu, T. J., and Hall, L. S.: Northern Lawn Hill Platform: Depth, structure  
752 and isochore mapping update, *Geoscience Australia Record 2018/47*, 75pp, Geoscience Australia, Canberra, 2018.

753 Broadbent, G. C., Myers, R. E., and Wright, J. V.: Geology and origin of shale-hosted Zn-Pb-Ag mineralization at the  
754 Century deposit, northwest Queensland, Australia, *Economic Geology*, 93, 1264-1294,  
755 10.2113/gsecongeo.93.8.1264, 1998.

756 Carr, G. R., Denton, G. J., Parr, J., Sun, S.-S., Korsch, R. J., and Boden, S. B.: Lightning does strike twice; multiple ore  
757 events in major mineralised systems in northern Australia, in: *Predictive mineral discovery under cover, extended*  
758 *abstracts*, edited by: Muhling, J., Goldfarb, R., Vielreicher, N., Bierlein, F., Stumpfl, E., Groves, D. I., and  
759 Kenworthy, S., Centre for Global Metallogeny, The University of Western Australia, Perth, 2004.

760 Carr, L. K., Southby, C., Henson, P., Costelloe, R., Anderson, J. R., Jarrett, A. J. M., Carson, C. J., MacFarlane, S. K.,  
761 Gorton, J., Hutton, L. J., Troup, A., Williams, B., Khider, K., Bailey, A. H. E., and Fomin, T.: Exploring for the future:  
762 South Nicholson Basin geological summary and seismic data interpretation. *Record 2019/21.*, Geoscience  
763 Australia, Canberra, 2019.

764 Cooke, D. R., Bull, S. W., Donovan, S., and Rogers, J. R.: K-metasomatism and base metal depletion in volcanic  
765 rocks from the McArthur Basin, Northern Territory—implications for base metal mineralization, *Economic Geology*,  
766 93, 1237–1263, 1998.

767 Cooper, M. A., Collins, D., Ford, M., Murphy, F. X., and Trayner, P. M.: Structural style, shortening estimates and  
768 the thrust front of the Irish Variscides, *Geological Society, London, Special Publications*, 14, 167-175,  
769 10.1144/gsl.sp.1984.014.01.16, 1984.

770 Cooper, M. A., Williams, G. D., de Graciansky, P. C., Murphy, R. W., Needham, T., de Paor, D., Stoneley, R., Todd, S.  
771 P., Turner, J. P., and Ziegler, P. A.: Inversion tectonics — a discussion, *Geological Society, London, Special*  
772 *Publications*, 44, 335-347, 10.1144/gsl.sp.1989.044.01.18, 1989.

773 Domagala, J., Southgate, P. N., McConachie, B. A., and Pidgeon, B. A.: Evolution of the Palaeoproterozoic Prize,  
774 Gun and lower Loretta supersequences of the Surprise Creek Formation and Mt Isa Group, *Australian Journal of*  
775 *Earth Sciences*, 47, 485 - 507, 2000.

776 Dooley, T., and McClay, K. R.: Analog modeling of pull-apart basins, *AAPG Bulletin*, 81, 1804-1826, 1997.

777 Duncan, R. J., Stein, H. J., Evans, K. A., Hitzman, M. W., Nelson, E. P., and Kirwin, D. J.: A new geochronological  
778 framework for mineralization and alteration in the Selwyn-Mount Dore corridor, eastern fold belt, Mount Isa

779 Inlier, Australia: Genetic implications for iron oxide copper-gold deposits, *Economic Geology*, 106, 169-192,  
780 10.2113/econgeo.106.2.169, 2011.

781 Foster, D. R. W., and Rubenach, M.: Isograd patterns and regional low-pressure- high-temperature metamorphism  
782 of pelitic, mafic and calc-silicate rocks along an east-west section through the Mount Isa Inlier, *Australian Journal*  
783 *of Earth Sciences*, 53, 167-186, 2006.

784 Foster, D. R. W., and Austin, J. R.: The 1800–1610 Ma stratigraphic and magmatic history of the eastern  
785 succession, Mount Isa Inlier, and correlations with adjacent Paleoproterozoic terranes, *Precambrian Research*,  
786 163, 7-30, <http://dx.doi.org/10.1016/j.precamres.2007.08.010>, 2008.

787 Frogtech Geoscience: North West Queensland SEEBASE® Study and GIS. Queensland Geological Record 2018/03,  
788 2018.

789 Gibson, G. M., Rubenach, M. J., Neumann, N. L., Southgate, P. N., and Hutton, L. J.: Syn- and post-extensional  
790 tectonic activity in the Palaeoproterozoic sequences of Broken Hill and Mount Isa and its bearing on  
791 reconstructions of Rodinia, *Precambrian Research*, 166, 350-369,  
792 <http://dx.doi.org/10.1016/j.precamres.2007.05.005>, 2008.

793 Gibson, G. M., Henson, P. A., Neumann, N. L., Southgate, P. N., and Hutton, L. J.: Paleoproterozoic-earliest  
794 Mesoproterozoic basin evolution in the Mount Isa region, northern Australia and implications for reconstructions  
795 of the Nuna and Rodinia supercontinents, *Episodes*, 35, 131-141, 2012.

796 Gibson, G. M., Meixner, A. J., Withnall, I. W., Korsch, R. J., Hutton, L. J., Jones, L. E. A., Holzschuh, J., Costelloe, R.  
797 D., Henson, P. A., and Saygin, E.: Basin architecture and evolution in the Mount Isa mineral province, northern  
798 Australia: Constraints from deep seismic reflection profiling and implications for ore genesis, *Ore Geology*  
799 *Reviews*, 76, 414-441, <http://dx.doi.org/10.1016/j.oregeorev.2015.07.013>, 2016.

800 Gibson, G. M., Hutton, L. J., and Holzschuh, J.: Basin inversion and supercontinent assembly as drivers of  
801 sediment-hosted Pb–Zn mineralization in the Mount Isa region, northern Australia, *Journal of the Geological*  
802 *Society*, 174, 773-786, 10.1144/jgs2016-105, 2017.

803 Gibson, G. M., Champion, D. C., Withnall, I. W., Neumann, N. L., and Hutton, L. J.: Assembly and breakup of the  
804 Nuna supercontinent: Geodynamic constraints from 1800 to 1600 Ma sedimentary basins and basaltic  
805 magmatism in northern Australia, *Precambrian Research*, 313, 148-169,  
806 <https://doi.org/10.1016/j.precamres.2018.05.013>, 2018.

807 Gibson, G. M., Champion, D. C., Huston, D. L., and Withnall, I. W.: Orogenesis in Paleo-Mesoproterozoic eastern  
808 Australia: A response to arc-continent and continent-continent collision during assembly of the Nuna  
809 supercontinent, *Tectonics*, 39, e2019TC005717, 10.1029/2019tc005717, 2020.

810 Giles, D., Betts, P. G., and Lister, G. S.: Far-field continental back-arc setting for the 1.8-1.67 Ga basins of north-  
811 east Australia, *Geology*, 30, 823-826, 2002.

812 Giles, D., Betts, P. G., and Lister, G. S.: 1.8–1.5 Ga links between the North and South Australian cratons and the  
813 early–middle Proterozoic configuration of Australia, *Tectonophysics*, 380, 27-41,  
814 <http://dx.doi.org/10.1016/j.tecto.2003.11.010>, 2004.

815 Giles, D., Betts, P. G., Ailleres, L., Hulscher, B., Hough, M., and Lister, G. S.: Evolution of the Isan Orogeny at the  
816 southeastern margin of the Mt Isa Inlier, *Australian Journal of Earth Sciences*, 53, 91-108, 2006.

817 Glikson, A. Y., Derrick, G. M., Wilson, I. H., and Hill, R. M.: Tectonic evolution and crustal setting of the middle  
818 Proterozoic Leichhardt River Fault Trough, Mount Isa region, northwest Queensland, *BMR Journal of Australian*  
819 *Geology and Geophysics*, 1, 115-129, 1976.

820 Glikson, M., Golding, S. D., and Southgate, P. N.: Thermal evolution of the ore-hosting Isa Superbasin: Central and  
821 northern Lawn Hill Platform, *Economic Geology*, 101, 1211-1229, 10.2113/gseconge.101.6.1211, 2006.

822 Golding, S. D., Uysal, I. T., Glikson, M., Baublys, K. A., and Southgate, P. N.: Timing and chemistry of fluid-flow  
823 events in the Lawn Hill Platform, northern Australia, *Economic Geology*, 101, 1231-1250,  
824 10.2113/gseconge.101.6.1231, 2006.

825 Gorton, J., and Troup, A.: Petroleum systems of the Proterozoic in northwest Queensland and a description of  
826 various play types, *The APPEA Journal*, 58, 311-320, <https://doi.org/10.1071/AJ17115>, 2018.

827 Hayward, A. B., and Graham, R. H.: Some geometrical characteristics of inversion, *Geological Society, London,*  
828 *Special Publications*, 44, 17-39, 10.1144/gsl.sp.1989.044.01.03, 1989.

829 Heinrich, C. A., Bain, J. H. C., Mernagh, T. P., Wyborn, L. A. I., Andrew, A. S., and Waring, C. L.: Fluid and mass  
830 transfer during metabasalt alteration and copper mineralisation at Mount Isa, Australia, *Economic Geology*, 90,  
831 705-730, 1995.

832 Hinman, M.: Base metal mineralisation at McArthur River: Structure and kinematics of the Hyc-Cooley Zone,  
833 Australian Geological Survey Organisation Record 1995/5, 41pp, 1995.

834 Holcombe, R. J., Pearson, P. J., and Oliver, N. H. S.: Geometry of a middle Proterozoic extensional decollement in  
835 north-eastern Australia, *Tectonophysics*, 191, 255-274, 1991.

836 Huston, D. L., Stevens, B., Southgate, P. N., Muhling, P., and Wyborn, L.: Australian Zn-Pb-Ag ore-forming systems:  
837 A review and analysis, *Economic Geology*, 101, 1117-1157, 10.2113/gsecongeo.101.6.1117, 2006.

838 Huston, D. L., Mernagh, T. P., Hagemann, S. G., Doublier, M. P., Fiorentini, M., Champion, D. C., Lynton Jaques, A.,  
839 Czarnota, K., Cayley, R., Skirrow, R., and Bastrakov, E.: Tectono-metallogenic systems — the place of mineral  
840 systems within tectonic evolution, with an emphasis on Australian examples, *Ore Geology Reviews*, 76, 168-210,  
841 <http://dx.doi.org/10.1016/j.oregeorev.2015.09.005>, 2016.

842 Hutton, L. J., and Sweet, I. P.: Geological evolution, tectonic style and economic potential of the Lawn Hill Platform  
843 cover, northwest Queensland, *BMR Journal of Australian Geology and Geophysics*, 7, 125-134, 1982.

844 Jackson, M. J., Powell, T. G., Summons, R. E., and Sweet, I. P.: Hydrocarbon shows and petroleum source rocks in  
845 sediments as old as  $1.7 \times 10^9$  years, *Nature*, 322, 727-729, 10.1038/322727a0, 1986.

846 Jackson, M. J., Scott, D. L., and Rawlings, D. J.: Stratigraphic framework for the Leichhardt and Calvert superbasins:  
847 Review and correlations of the pre- 1700 Ma successions between Mt Isa and McArthur River, *Australian Journal  
848 of Earth Sciences*, 47, 381-403, 10.1046/j.1440-0952.2000.00789.x, 2000.

849 Jarrett, A. J. M., Cox, G. M., Southby, C., Hong, Z., Palatty, P., Carr, L., and Henson, P.: Source rock geochemistry of  
850 the McArthur Basin, northern Australia: Rock-eval pyrolysis data release. Record 2018/24. Geoscience Australia,  
851 Canberra, <http://dx.doi.org/10.11636/Record.2018.024>, 2018.

852 Kesler, S. E., Jones, H. D., Furman, F. C., Sassen, R., Anderson, W. H., and Kyle, J. R.: Role of crude oil in the genesis  
853 of Mississippi Valley-type deposits: Evidence from the Cincinnati Arch, *Geology*, 22, 609-612, 10.1130/0091-  
854 7613(1994)022<0609:rocoit>2.3.co;2, 1994.

855 Korsch, R. J., Huston, D. L., Henderson, R. A., Blewett, R. S., Withnall, I. W., Fergusson, C. L., Collins, W. J., Saygin,  
856 E., Kositcin, N., Meixner, A. J., Chopping, R., Henson, P. A., Champion, D. C., Hutton, L. J., Wormald, R., Holzschuh,  
857 J., and Costelloe, R. D.: Crustal architecture and geodynamics of north Queensland, Australia: Insights from deep  
858 seismic reflection profiling, *Tectonophysics*, 572-573, 76-99, <http://dx.doi.org/10.1016/j.tecto.2012.02.022>, 2012.

859 Kositcin, N., and Carson, C. J.: New shrimp U-Pb zircon ages from the South Nicholson and Carrara Range region,  
860 Northern Territory. Record 2019/09. Geoscience Australia, Canberra., 2019.

861 Krassay, A. A., Bradshaw, B. E., Domagala, J., and Jackson, M. J.: Siliciclastic shoreline to growth-faulted, turbiditic  
862 sub-basins: The Proterozoic River Supersequence of the upper McNamara Group on the Lawn Hill Platform,  
863 northern Australia, *Australian Journal of Earth Sciences*, 47, 533 - 562, 2000a.

864 Krassay, A. A., Domagala, J., Bradshaw, B. E., and Southgate, P. N.: Lowstand ramps, fans and deep-water  
865 Palaeoproterozoic and Mesoproterozoic facies of the Lawn Hill Platform: The Term, Lawn, Wide and Doom  
866 supersequences of the Isa Superbasin, northern Australia, *Australian Journal of Earth Sciences*, 47, 563 - 597,  
867 2000b.

868 Kunzmann, M., Schmid, S., Blaikie, T. N., and Halverson, G. P.: Facies analysis, sequence stratigraphy, and carbon  
869 isotope chemostratigraphy of a classic Zn-Pb host succession: The Proterozoic middle McArthur Group, McArthur  
870 Basin, Australia, *Ore Geology Reviews*, 106, 150-175, <https://doi.org/10.1016/j.oregeorev.2019.01.011>, 2019.

871 Large, R. R., Bull, S. W., McGoldrick, P. J., Walters, S., Derrick, G. M., and Carr, G. R.: Stratiform and strata-bound  
872 Zn-Pb-Ag deposits in Proterozoic sedimentary basins, northern Australia, *Economic Geology 100th Anniversary  
873 Volume*, 931-963, 2005.

874 Leach, D. L., Bradley, D., Lewchuk, M. T., Symons, D. T., de Marsily, G., and Brannon, J.: Mississippi Valley-type  
875 lead-zinc deposits through geological time: Implications from recent age-dating research, *Miner Deposita*, 36,  
876 711-740, 10.1007/s001260100208, 2001.

877 Leach, D. L., Bradley, D. C., Huston, D., Pisarevsky, S. A., Taylor, R. D., and Gardoll, S. J.: Sediment-hosted lead-zinc  
878 deposits in earth history, *Economic Geology*, 105, 593-625, 10.2113/gsecongeo.105.3.593, 2010.

879 Lowell, J. D.: Mechanics of basin inversion from worldwide examples, *Geological Society, London, Special  
880 Publications*, 88, 39-57, 10.1144/gsl.sp.1995.088.01.04, 1995.

881 Martínez, F., Arriagada, C., Mpodozis, C., and Peña<sup>1</sup>, M.: The Lautaro Basin: A record of inversion tectonics in  
882 northern Chile, *Andean Geology*, 39, 258-278, 2012.

883 McClay, K. R.: The geometries and kinematics of inverted fault systems: A review of analogue model studies,  
884 Geological Society, London, Special Publications, 88, 97-118, 10.1144/gsl.sp.1995.088.01.07, 1995.

885 McClay, K. R., and White, M. J.: Analogue modelling of orthogonal and oblique rifting, *Marine and Petroleum*  
886 *Geology*, 12, 137-151, 1995.

887 McClay, K. R., Dooley, T., Whitehouse, P., and Mills, M.: 4-D evolution of rift systems: Insights from scaled physical  
888 models, *AAPG Bulletin*, 86, 935-959, 10.1306/61eedbf2-173e-11d7-8645000102c1865d, 2002.

889 McConachie, B. A., Barlow, M. G., Dunster, J. N., Meaney, R. A., and Schaap, A. D.: The Mount Isa basin-definition,  
890 structure and petroleum geology, *APEA Journal*, 33, 237-257, 1993.

891 McConachie, B. A., and Dunster, J. N.: Sequence stratigraphy of the Bowthorn block in the northern Mount Isa  
892 basin, Australia: Implications for the base-metal mineralization process, *Geology*, 24, 155-158, 10.1130/0091-  
893 7613(1996)024<0155:ssotbb>2.3.co;2, 1996.

894 McGoldrick, P., Winefield, P., Bull, S., Selley, D., and Scott, R. J.: Sequences, synsedimentary structures, and sub-  
895 basins: The where and when of sedex zinc systems in the southern McArthur Basin, Australia, *Society of Economic*  
896 *Geologists*, Special Publication 15, 367-389, 2010.

897 Neumann, N. L., Southgate, P. N., Gibson, G. M., and McIntyre, A.: New shrimp geochronology for the western  
898 fold belt of the Mount Isa Inlier: Developing a 1800-1650 Ma event framework, *Australian Journal of Earth*  
899 *Sciences*, 53, 1023-1039, 2006.

900 Neumann, N. L., Gibson, G. M., and Southgate, P. N.: New shrimp age constraints on the timing and duration of  
901 magmatism and sedimentation in the Mary Kathleen Fold Belt, Mt Isa Inlier, *Australian Journal of Earth Sciences*,  
902 56, 965-983, 2009.

903 O'Dea, M. G., Lister, G. S., Betts, P. G., and Pound, K. S.: A shortened intraplate rift system in the Proterozoic  
904 Mount Isa terrane, N. W. Queensland, Australia, *Tectonics*, 16, 425-441, 1997a.

905 O'Dea, M. G., Lister, G. S., MacCready, T., Betts, P. G., Oliver, N. H. S., Pound, K. S., Huang, W., Valenta, R. K.,  
906 Oliver, N. H. S., and Valenta, R. K.: Geodynamic evolution of the Proterozoic Mount Isa terrain, Geological Society,  
907 London, Special Publications, 121, 99-122, 10.1144/gsl.sp.1997.121.01.05, 1997b.

908 Page, R. W., and Sun, S. S.: Aspects of geochronology and crustal evolution in the eastern fold belt, Mt Isa Inlier,  
909 *Australian Journal of Earth Sciences*, 45, 343-361, 10.1080/08120099808728396, 1998.

910 Page, R. W., Jackson, M. J., and Krassay, A. A.: Constraining sequence stratigraphy in north Australian basins:  
911 Shrimp U-Pb zircon geochronology between Mt Isa and McArthur River, *Australian Journal of Earth Sciences*, 47,  
912 431 - 459, 2000.

913 Pearson, P. J., Holcombe, R. J., and Page, R. W.: Synkinematic emplacement of the middle Proterozoic Wonga  
914 Batholith into a midcrustal shear zone, Mount Isa Inlier, Queensland, Australia, in: *Detailed studies of the Mount*  
915 *Isa Inlier: Australian Geological Survey Organisation Bulletin 243*, edited by: Stewart, A. J., and Blake, D. H.,  
916 Canberra, 289-328, 1991.

917 Polito, P. A., Kyser, T. K., Golding, S., D., and Southgate, P. N.: Zinc deposits and related mineralization of the  
918 Burketown mineral field, including the world-class Century deposit, northern Australia: Fluid inclusion and stable  
919 isotope evidence for basin fluid sources, *Economic Geology*, 101, 1251-1273, 10.2113/gsecongeo.101.6.1251,  
920 2006.

921 Pollard, P., and McNaughton, N. J.: U/Pb geochronology and Sm/Nd isotope characterization of Proterozoic  
922 intrusive rocks in the Cloncurry district, Mount Isa Inlier, Australia. *Amira P438 Cloncurry base metals and gold*  
923 *final report: Section 4*, 19pp., 1997.

924 Pollard, P. J., Mark, G., and Mitchell, L. C.: Geochemistry of post-1540 Ma granites spatially associated with  
925 regional sodic-calcic alteration and Cu-Au-Co mineralisation, Cloncurry district, northwest Queensland *Economic*  
926 *Geology*, 93, 1330-1344, 1998.

927 Pourteau, A., Smit, M. A., Li, Z.-X., Collins, W. J., Nordsvan, A. R., Volante, S., and Li, J.: 1.6 Ga crustal thickening  
928 along the final Nuna suture, *Geology*, 46, 959-962, 10.1130/G45198.1, 2018.

929 Pursuit Minerals: Pursuit Minerals Limited lists on ASX and immediately commences Bluebush drilling program.  
930 [Http://pursuitminerals.Com.Au/wp-content/uploads/2017/09/pur-lists-on-ASX-and-commences-Bluebush-](http://pursuitminerals.Com.Au/wp-content/uploads/2017/09/pur-lists-on-ASX-and-commences-Bluebush-drilling-program.Pdf)  
931 [drilling-program.Pdf](http://pursuitminerals.Com.Au/wp-content/uploads/2017/09/pur-lists-on-ASX-and-commences-Bluebush-drilling-program.Pdf), 2017.

932 Rawlings, D. J., Sweet, I. P., and Kruse, P. D.: Mount Drummond, Northern Territory. 1:250 000 geological map  
933 series explanatory notes, SE 53-12. Northern Territory Geological Survey, Darwin, 2008.

934 Rohrlach, B. D., Fu, M., and Clarke, J. D. A.: Geological setting, paragenesis and fluid history of the Walford Creek  
935 Zn-Pb-Cu-Ag prospect, Mt Isa basin, Australia, *Australian Journal of Earth Sciences*, 45, 63-81,  
936 10.1080/08120099808728367, 1998.

937 Rubenach, M. J., Foster, D. R. W., Evins, P. M., Blake, K. L., and Fanning, C. M.: Age constraints on the  
938 tectonothermal evolution of the Selwyn zone, eastern fold belt, Mount Isa Inlier, *Precambrian Research*, 163, 81-  
939 107, 2008.

940 Scott, D. L., Bradshaw, B. E., and Tarlowski, C. Z.: The tectonostratigraphic history of the Proterozoic northern  
941 Lawn Hill Platform, Australia: An integrated intracontinental basin analysis, *Tectonophysics*, 300, 329-358,  
942 [https://doi.org/10.1016/S0040-1951\(98\)00253-4](https://doi.org/10.1016/S0040-1951(98)00253-4), 1998.

943 Scott, D. L., Rawlings, D. J., Page, R. W., Tarlowski, C. Z., Idnurm, M., Jackson, M. J., and Southgate, P. N.:  
944 Basement framework and geodynamic evolution of the Palaeoproterozoic superbasins of north-central Australia:  
945 An integrated review of geochemical, geochronological and geophysical data, *Australian Journal of Earth Sciences*,  
946 47, 341 - 380, 2000.

947 Southgate, P. N., Bradshaw, B. E., Domagala, J., Jackson, M. J., Idnurm, M., Krassay, A. A., Page, R. W., Sami, T. T.,  
948 Scott, D. L., Lindsay, J. F., McConachie, B. A., and Tarlowski, C.: Chronostratigraphic basin framework for  
949 Palaeoproterozoic rocks (1730-1575 Ma) in northern Australia and implications for base-metal mineralisation,  
950 *Australian Journal of Earth Sciences*, 47, 461 - 483, 2000a.

951 Southgate, P. N., Scott, D. L., Sami, T. T., Domagala, J., Jackson, M. J., James, N. P., and Kyser, T. K.: Basin shape  
952 and sediment architecture in the Gun Supersequence: A strike-slip model for Pb-Zn-Ag ore genesis at Mt Isa,  
953 *Australian Journal of Earth Sciences*, 47, 509 - 531, 2000b.

954 Southgate, P. N., Kyser, T. K., Scott, D. L., Large, R. R., Golding, S. D., and Polito, P. A.: A basin system and fluid-  
955 flow analysis of the Zn-Pb-Ag Mount Isa-type deposits of northern Australia: Identifying metal source, basinal  
956 brine reservoirs, times of fluid expulsion, and organic matter reactions, *Economic Geology*, 101, 1103-1115,  
957 10.2113/gsecongeo.101.6.1103, 2006.

958 Southgate, P. N., Neumann, N. L., and Gibson, G. M.: Depositional systems in the Mt Isa inlier from 1800 Ma to  
959 1640 Ma: Implications for Zn–Pb–Ag mineralisation, *Australian Journal of Earth Sciences*, 60, 157-173, 2013.

960 Sweet, I. P.: Carrara Range region NT Geological Map Commentary. Record 6460. , Geoscience Australia,  
961 Canberra, 1984.

962 Sweet, I. P.: The geology of the South Nicholson Group, northwest Queensland. *Queensland Geological Record*  
963 2017/07, 2017.

964 Thomas, D. W., and Coward, M. P.: Late Jurassic-early Cretaceous inversion of the northern east Shetland Basin,  
965 northern North Sea, *Geological Society, London, Special Publications*, 88, 275-306, 10.1144/gsl.sp.1995.088.01.16,  
966 1995.

967 Turner, J. P., and Williams, G. A.: Sedimentary basin inversion and intra-plate shortening, *Earth-Science Reviews*,  
968 65, 277-304, <https://doi.org/10.1016/j.earscirev.2003.10.002>, 2004.

969 Withnall, I. W.: Geochemistry and tectonic significance of Proterozoic mafic rocks from the Georgetown Inlier,  
970 north Queensland, *BMR Journal of Australian Geology & Geophysics*, 9, 339-351, 1985.

971 Withnall, I. W., and Hutton, L. J.: Chapter 2: North Australian Craton, in: *Geology of Queensland*, edited by: Jell, P.  
972 A., Geological Survey of Queensland, Brisbane, 23-112, 2013.

973 Yang, B., Collins, A. S., Cox, G. M., Jarrett, A. J. M., Denyszyn, S., Blades, M. L., Farkaš, J., and Glorie, S.: Using  
974 Mesoproterozoic sedimentary geochemistry to reconstruct basin tectonic geography and link organic carbon  
975 productivity to nutrient flux from a northern Australian large igneous province, *Basin Research*, n/a,  
976 10.1111/bre.12450, 2020.

977 Yang, J., and Radulescu, M.: Paleo-fluid flow and heat transport at 1575 Ma over an E–W section in the northern  
978 Lawn Hill Platform, Australia: Theoretical results from finite element modeling, *Journal of Geochemical*  
979 *Exploration*, 89, 445-449, <https://doi.org/10.1016/j.gexplo.2005.11.079>, 2006.

980

## 981 **Figure Captions**

982 Figure 1. (a) Simplified geological map for northern Australia showing principal tectono-morphological  
983 elements and Pb–Zn mineral deposits (after Jackson et al., 2000). (b) More detailed geological map of  
984 periclinal folds developed in stratigraphy of the inverted Isa Superbasin on the Lawn Hill Platform  
985 northeast of Century Mine and seismic reflection lines 06GA–M1 and 06GA–M2 along which these  
986 structures are imaged. Figure reproduced with permission under the Creative Commons Attribution 4.0  
987 International Licence: <http://creativecommons.org/licenses/by/4.0/legalcode>. © Commonwealth of  
988 Australia (Geoscience Australia) 2020.

989 Figure 2. Map showing presently defined limits of outcropping Leichhardt, Calvert and Isa superbasins  
990 across the Mount Isa region. Seismic reflection data indicate that all three basins are variably preserved in  
991 the subsurface geology beneath the South Nicholson and Georgina basins and continue northwards into the  
992 McArthur Basin and Batten Trough (see Carr et al., 2019). Reproduced with permission: Licensed CC BY  
993 version 4.0 © State of Queensland, 2020.

994 Figure 3. Simplified stratigraphic column for Mount Isa region and neighbouring southern McArthur  
995 Basin showing three-fold subdivision into Leichhardt, Calvert and Isa superbasins but different  
996 interpretations of basin history and tectonic evolution (Betts and Lister, 2001; Betts et al., 2003; Gibson et  
997 al., 2016; Southgate et al., 2000a). The Carrara Range Group is shown as part of the lower Tawallah  
998 Group and a correlative of the Leichhardt Superbasin based on revised geological mapping (Rawlings et  
999 al., 2008) and recently published geochronological data (Kositcin and Carson, 2019) for the McArthur  
1000 Basin. Vertical blue lines represent periods of non-deposition or missing geological record; open circles =  
1001 basal conglomerates; vvv = basaltic volcanic rocks. Individual Pb–Zn deposits are shown as yellow stars:  
1002 1= Mount Isa; 2=Lady Loretta; 3=McArthur River; 4=Century.

1003 Figure 4. South Nicholson seismic grid and late Paleoproterozoic–early Mesoproterozoic basinal sequences  
1004 draped over gravity image for western extension of the Lawn Hill Platform into Northern Territory. Note  
1005 anomalously deep gravity low centred on the Carrara Sub-basin (Carr et al., 2019) which is bounded by the  
1006 Carrara Range (gravity high) to the north of line 17GA–SN1. Geology modified from Rawlings et al. (2008)  
1007 and Ahmad & Munson (2013). Gravity image reproduced with permission under the Creative Commons  
1008 Attribution 4.0 International Licence: <http://creativecommons.org/licenses/by/4.0/legalcode>. ©  
1009 Commonwealth of Australia (Geoscience Australia) 2020.

1010 Figure 5. Basin and basement architecture for northern Lawn Hill Platform showing main depocentres,  
1011 fault trends and depth to magnetic basement for Isa Superbasin (after Gorton and Troup, 2018 from image  
1012 created by Frogtech Geoscience, 2018). Seismic lines are shown in various colours and include the 1994  
1013 (Comalco) and 2011 (Teck Resources) industry surveys across the Isa Superbasin and adjacent Punjab  
1014 Structure (P). Yellow lines are for composite image presented in Figures 6–7. Note compartmentalisation  
1015 of depocentres brought about by interference between the ENE and NW-trending faults; latter are of  
1016 Calvert age and include older normal faults (e.g. Riversleigh Fault) reactivated as strike-slip structures  
1017 during crustal extension accompanying formation of the Isa Superbasin. Figure is reproduced with  
1018 permission under the Creative Commons Attribution 4.0 International Licence:  
1019 <http://creativecommons.org/licenses/by/4.0/legalcode>. © State Government of Queensland (Geological  
1020 Survey of Queensland, Georesources Division, Department of Natural Resources, Mines and Energy)  
1021 2020.

1022 Figure 6. North-south oriented transect across Lawn Hill Platform made up of selected industry and  
1023 government seismic sections (Fig. 5) showing predominance of north-dipping normal faults on which there  
1024 has been successive episodes of basin inversion, leaving behind a legacy of fault reactivation and periclinal  
1025 folding in (a) Punjab Structure and (b) Mount Caroline and Ploughed Mountain (after Gibson et al., 2017;  
1026 2020). Note thinning of River and Term supersequences northward through onlap in (a); the underlying

1027 Loretta Supersequence similarly thins northward but is bounded top and bottom by truncated surfaces  
1028 thought to reflect considerable loss of stratigraphic section by uplift and erosion accompanying the  
1029 1650–1640 Ma Riversleigh Tectonic Event. Sedimentary patterns point to growth faulting on north-dipping  
1030 structures during deposition of the Isa, but not underlying Calvert Superbasin whose sequences are merely  
1031 offset. Bluewater, Boga and Tin Tank Fault names adopted from Bradshaw et al (2018) and unpublished  
1032 industry maps (Pursuit Minerals, 2017). In (b) the older sequence had already been folded before the River  
1033 Supersequence was deposited as evidenced by thinning of the latter over the crests of folds developed in  
1034 the Calvert Superbasin at deeper levels beneath Mount Caroline. The Calvert Superbasin is, in turn,  
1035 separated by an angular unconformity from an even older underlying sequence inferred (Gibson et al.,  
1036 2017;Gibson et al., 2016) to be the Leichhardt Superbasin. Colour coding is same as Figure 3.

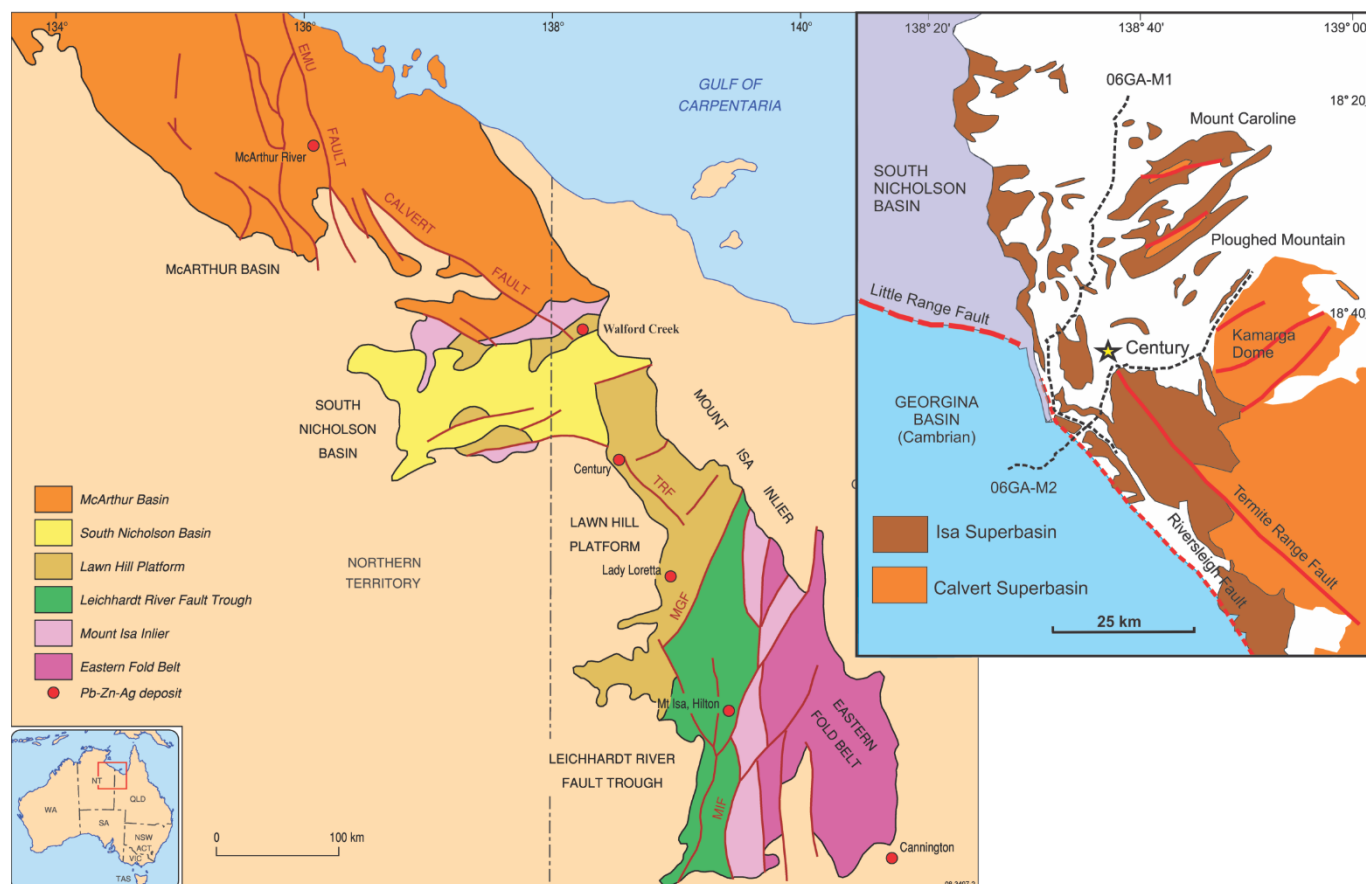
1037 Figure 7. West-east oriented seismic transects through northern Lawn Hill Platform. Westward thickening  
1038 of Calvert-age sedimentary units in both (a) and (b) is consistent with growth faulting on east-dipping  
1039 normal faults which have since been variably reactivated (Isa Orogeny). Conversely, no such growth is  
1040 obviously developed in the overlying Isa Superbasin whose lithological strike and inversion structures are  
1041 essentially parallel to the line of section. These units still thicken into the centre of the Isa Superbasin but  
1042 in a direction orthogonal to normal faults active during its deposition. Such faults, if imaged, would be  
1043 expected to be flat-lying or have very shallow dips parallel or subparallel to bedding in both sections rendering  
1044 their recognition very difficult. Some of the disruption to bedding in (b) along line 90Bn10 may be due to  
1045 such faults but overall the most obvious structural feature in the section is the broad arching and folding of  
1046 stratigraphy in the middle of the section consistent with imaging of an inversion fold in longitudinal cross-  
1047 section. Note truncated surface and angular unconformity at base of Loretta Supersequence in both sections  
1048 which is interpreted here to be an expression of basin inversion linked to the 1650-1640 Ma Riversleigh  
1049 Tectonic Event.

1050 Figure 8. West-east oriented section through (a) Century Mine (06GA–M2); (b) its western continuation  
1051 (17GA–SN1) across the South Nicholson Basin and Carrara Sub-basin (Carr et al., 2019); and (c) enlarged  
1052 section of 17GA–SN1 showing angular unconformity between Isa Superbasin and an underlying, variably  
1053 truncated older basin sequence. This older basin sequence directly overlies crystalline basement and likely  
1054 comprises rocks of the Leichhardt Superbasin, correlatives of which (Carrara Range Group) are exposed in  
1055 the Carrara Range immediately to the north of seismic line 17GA–SN1 (see Fig. 4). Note also that this older  
1056 sequence is contiguous with rocks in the Century region (06GA–M2) previously identified as part of the  
1057 Leichhardt Superbasin (Gibson et al., 2017). Conversely, the Calvert Superbasin is missing west of the  
1058 Riversleigh Fault consistent with non-deposition or a period of uplift and erosion during the course of which  
1059 it and a significant amount of the underlying Leichhardt Superbasin were removed from the geological  
1060 record.

1061 Figure 9. North-south oriented seismic sections west of Lawn Hill Platform showing shallow crystalline  
1062 basement and same basement-rooted inversion structure. Note major basement structure in (a) that cuts  
1063 downward all the way to the MOHO is probably the same basement structure/fault zone (Little Range Fault  
1064 Zone) imaged in (b) and over which all older sedimentary basins have been eroded so that rocks of  
1065 Cambrian age (Georgina Basin) directly overlie basement (17GA–SN4). Rocks of the South Nicholson  
1066 have similarly been removed for the crest of this basement block in 17GA–SN4 and, together with rocks of  
1067 the Isa Superbasin, increase in thickness northwards. The Isa Superbasin is abruptly truncated by the  
1068 basement structures and other subvertical structures suggestive of a flower structure and late-stage onset of  
1069 strike-slip faulting at or before deposition of Cambrian Georgina Basin.

1070 Figure 10. Basin inversion and resulting styles of structural architecture to be anticipated during crustal  
1071 shortening (after Martinez et al, 2012; McClay, 1995): (a) early normal fault; (b) harpoon structure from

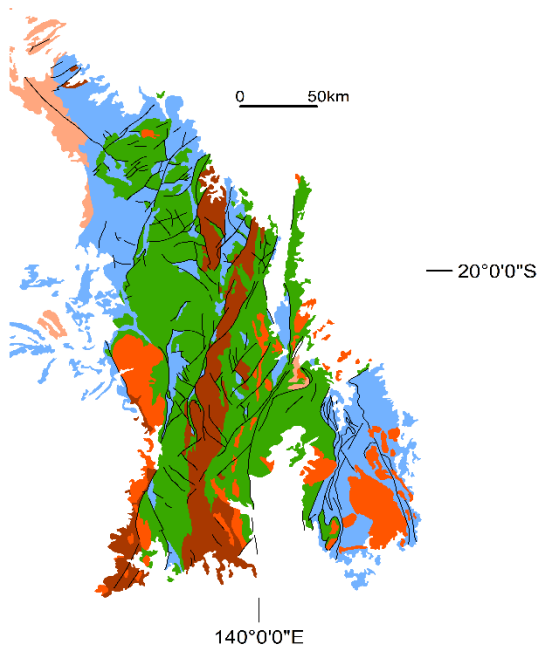
1072 partially inverted normal fault; (c) buttressing; (d) hangingwall is faulted forming hangingwall shortcut; (e)  
 1073 footwall shortcut thrust; (f) folding and truncation of normal fault by younger thrust; (g) thrust ramp above  
 1074 normal fault.



1075

1076 Figure 1

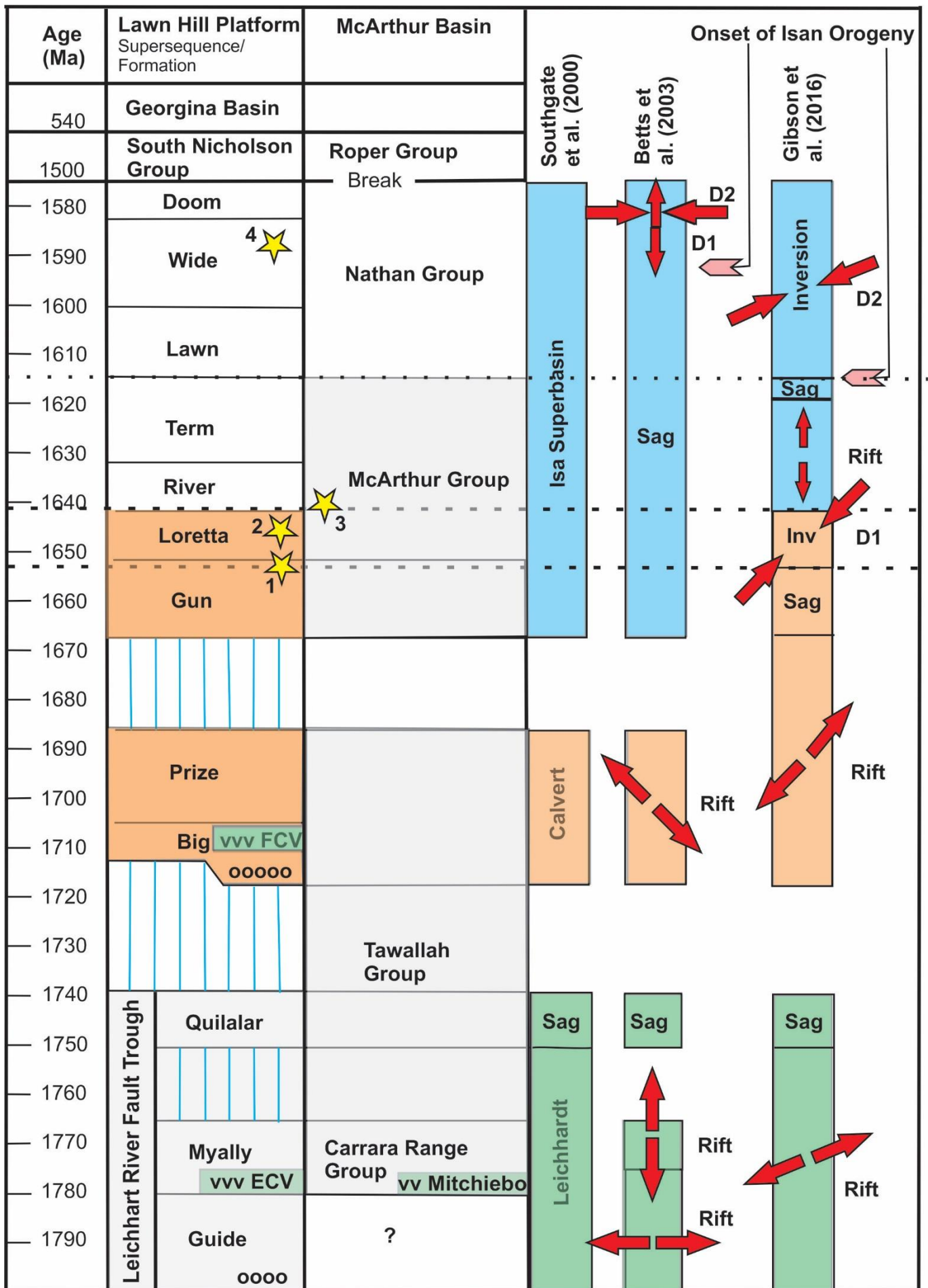




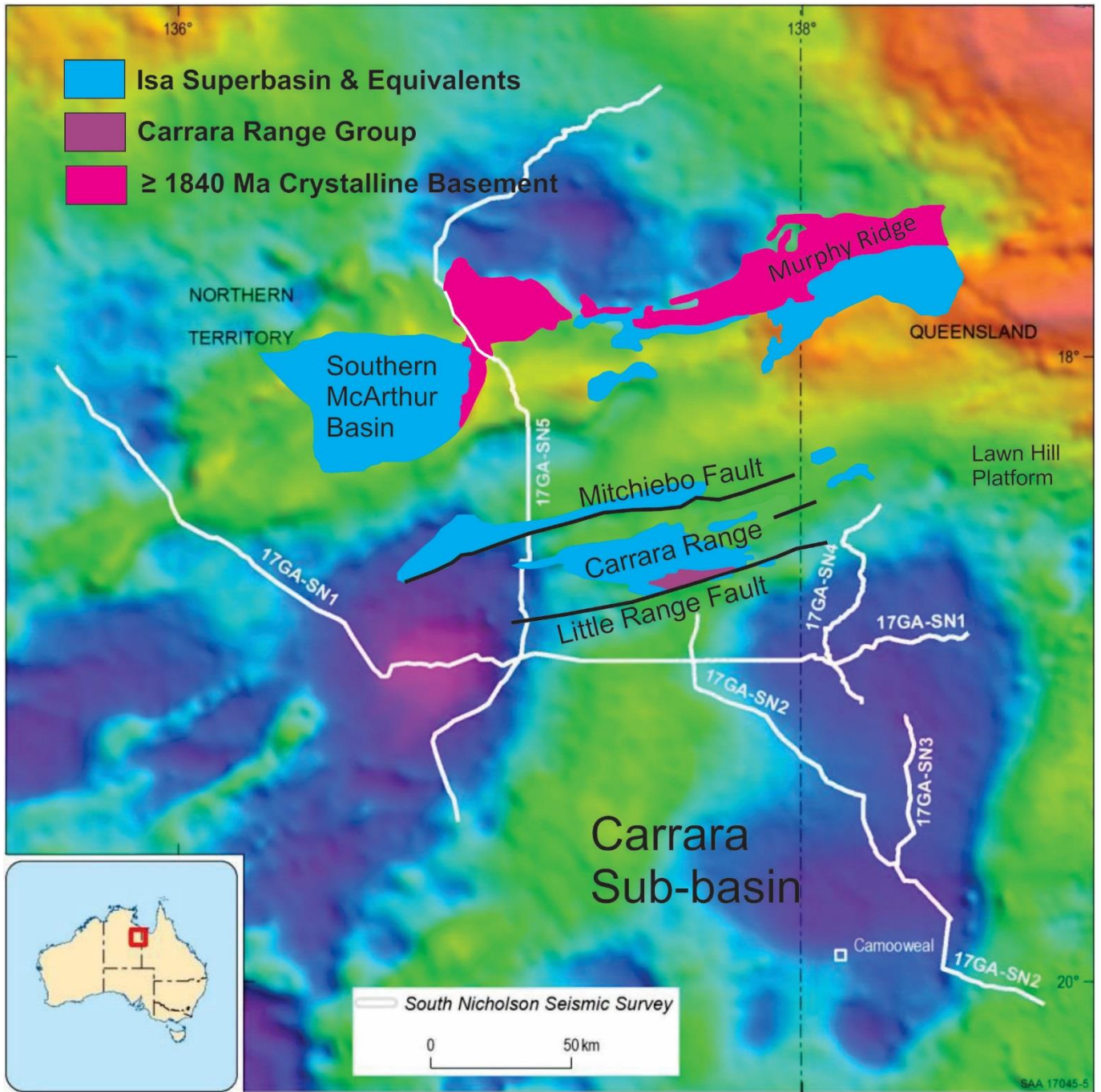
- Plutonic Suites
- Isa Superbasin
- Calvert Superbasin
- Leichhardt Superbasin
- pre-Leichhardt basement

1077

1078 Figure 2

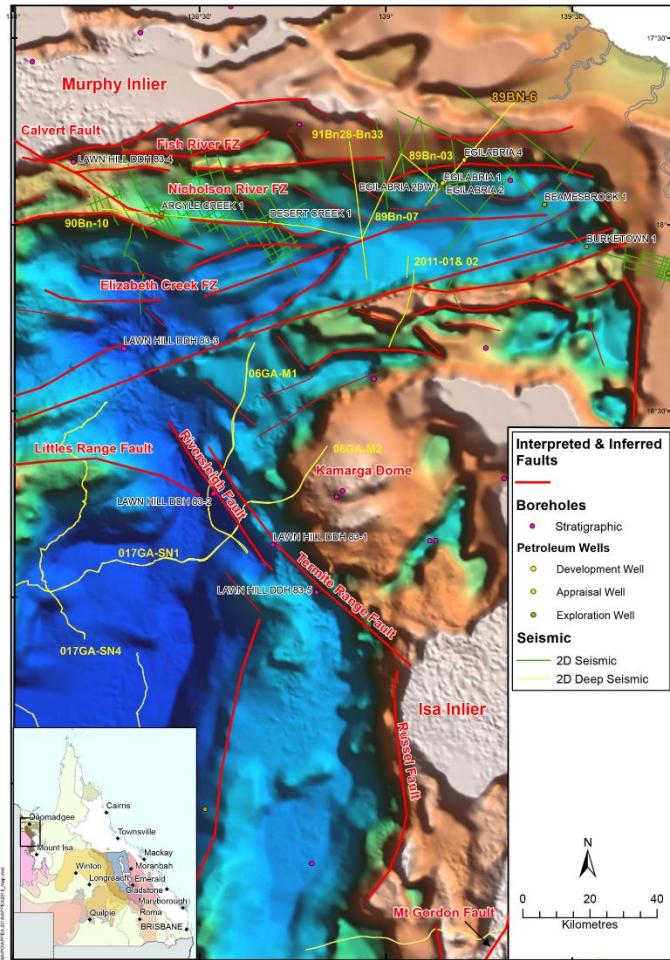


1080 Figure 3



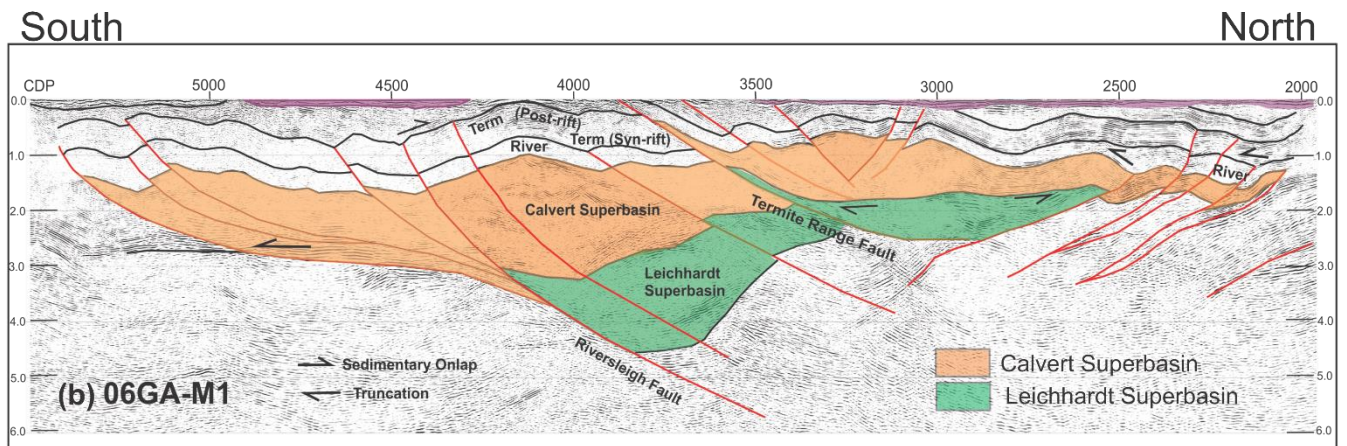
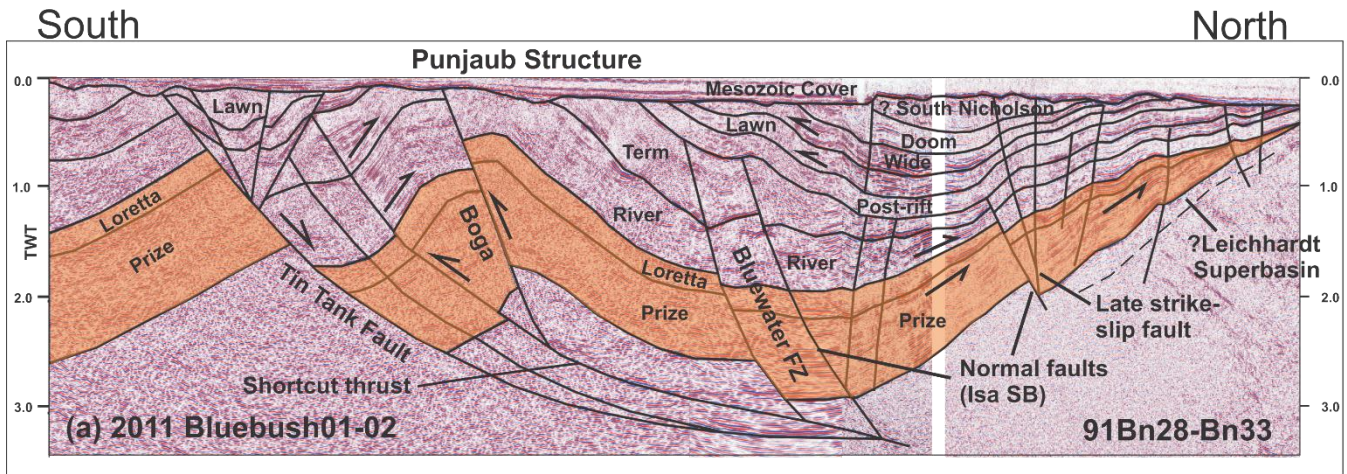
1081

1082 Figure 4



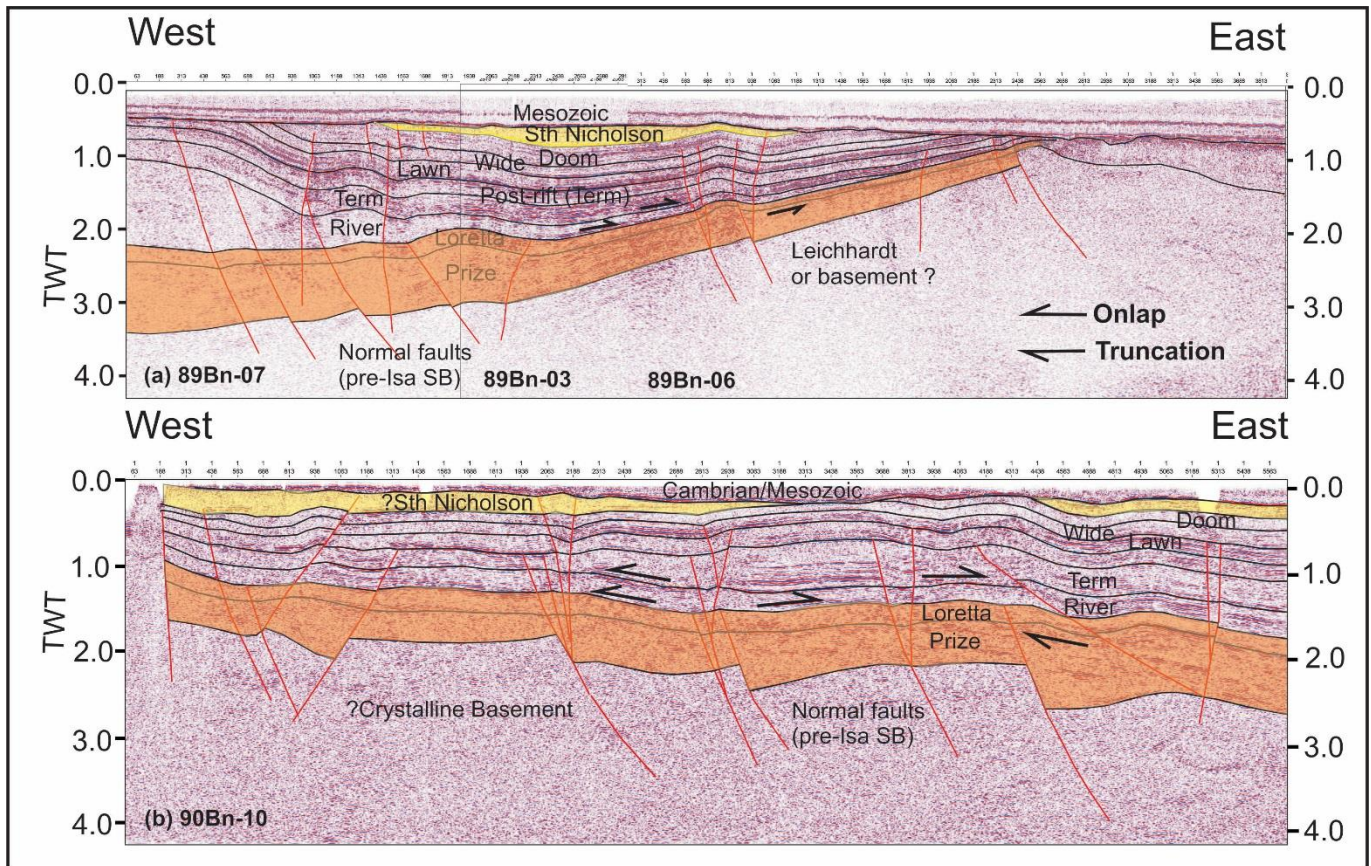
1083

1084 Figure 5



1085  
1086

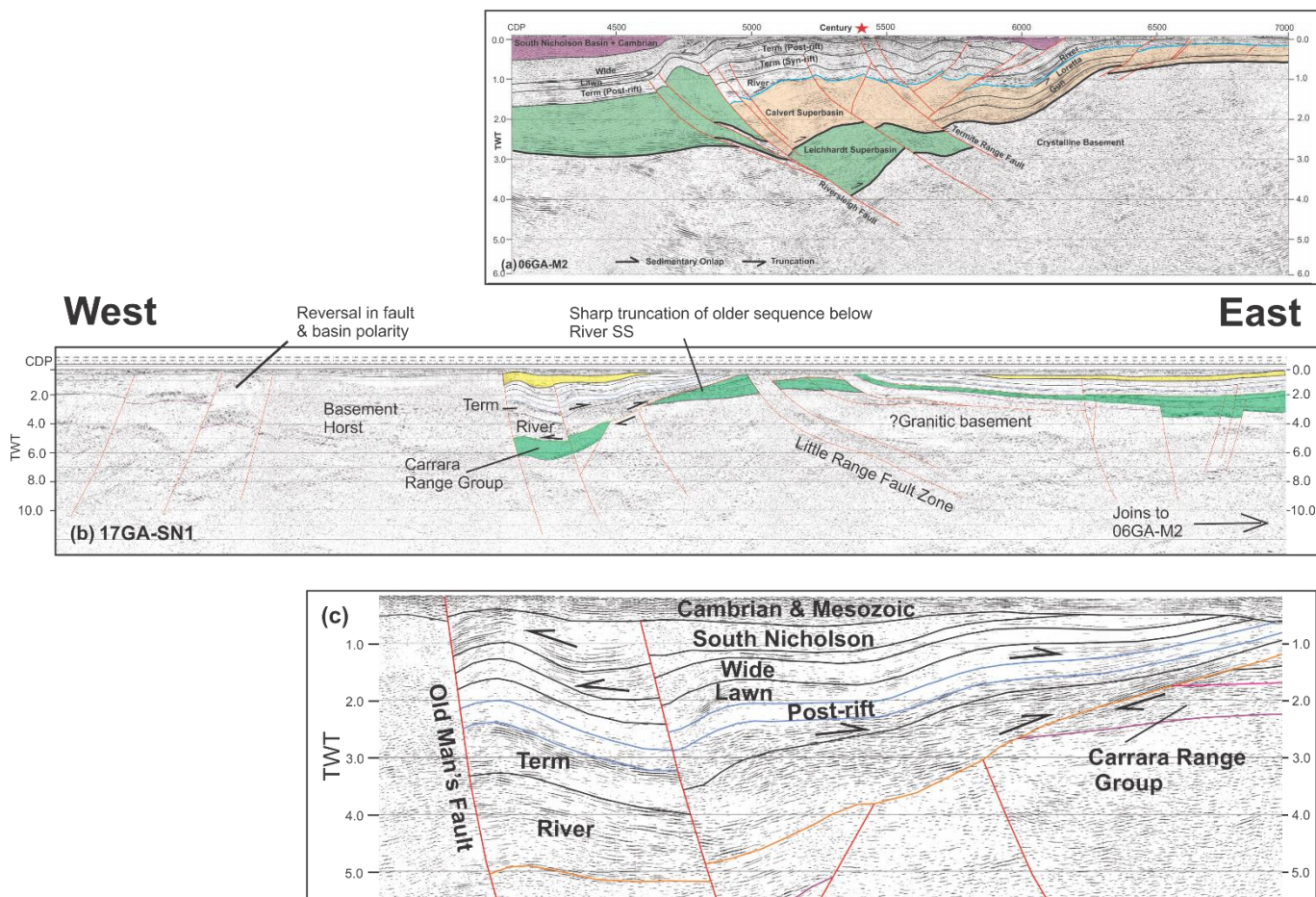
Figure 6



1087

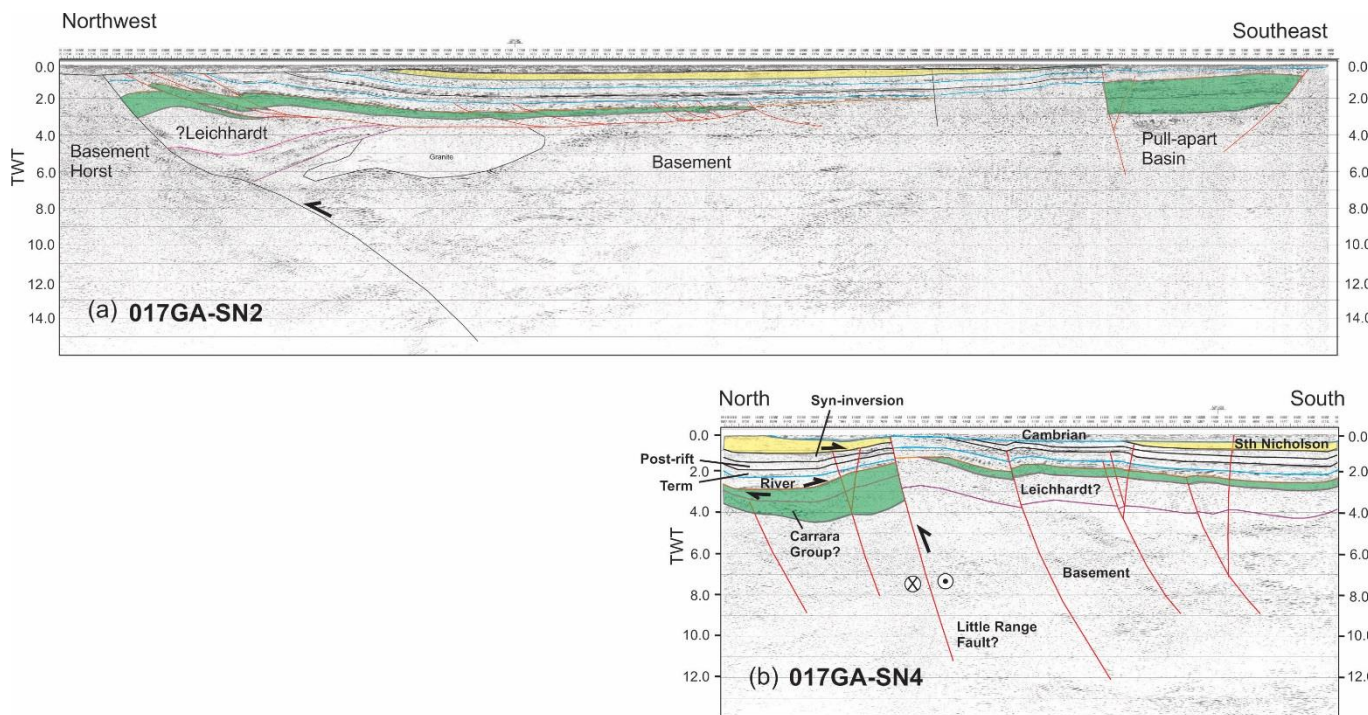
1088 Figure 7

1089



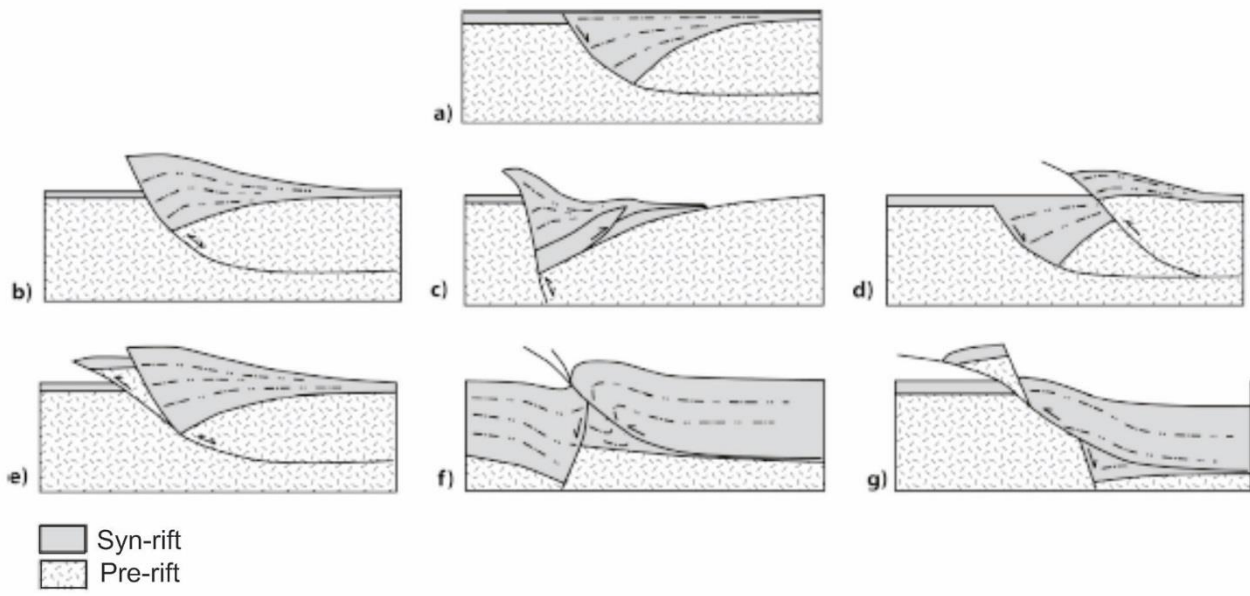
1090

1091 Figure 8



1092

1093 Figure 9



1094

1095 Figure 10